Structure and Reactivity of Free Arylium Ions. 2. Reactions of Decay-Formed Isomeric $XC_6H_4^+$ Ions with Gaseous and Liquid Nucleophiles

A. Filippi,[†] G. Lilla,[†] G. Occhiucci,[†] C. Sparapani,[†,‡] O. Ursini,[†] and M. Speranza*,[§]

Istituto di Chimica Nucleare del CNR, Area della Ricerca CNR di Roma, Rome, Italy, and the Dipartimento di Studi di Chimica e Tecnologia delle Sostanze Biologicamente Attive, Università di Roma "La Sapienza", Rome, Italy

Received October 7, 1994[⊗]

Labeled arylium ions $XC_6H_4^+$ (X = NO_2, CN, Cl, Br, OH, OCH_3) (*ortho*, 40%; *meta*, 40%; *para*, 20%) from the decay of uniformly multitritiated arenes XC_6H_5 have been allowed to react with methanol in the liquid and gaseous phase (P = 5–65 Torr) and with methyl halides in the gas phase (P = 10–760 Torr) at room temperature. The isomeric composition of the products from $O_2NC_6H_4^+$, characterized by a pronounced depletion of the *ortho* isomers, is regarded as due to effective singlet-carbenic to biradicalic state crossing in *o*-$O_2NC_6H_4^+$, favored by proximity between a lone pair of the NO_2 substituent and the formally vacant orbital. The same process is prevented in *o*-$NCC_6H_4^+$ by unfavorable arrangement of the corresponding orbitals. Nuclear decay of XC_6H_5 (X = Cl, Br, OCH_3) in liquid CH_3OH generates the corresponding methoxy derivatives in proportions reflecting those of their corresponding $XC_6H_4^+$ precursors (*ortho*:*meta*:*para* = 2:2:1). The specific solvation mode in *o*-$HOC_6H_4^+$ allows instead its extremely fast conversion to phenoxenium ion $C_6H_5O^+$, prior to addition to CH_3OH. The nature and the isomeric composition of the labeled products formed in gaseous CH_3OH (5–65 Torr) and methyl halides (10–760 Torr) point to $XC_6H_4^+$ ions (X = Cl, Br) with no tendency to undergo ring-hydrogen migration. In $HOC_6H_4^+$ ions, instead, intramolecular 1,2-hydrogen transfers readily take place whose phenomenological rate constants have been evaluated. In $CH_3OC_6H_4^+$ ions, the same process is obscured by a rapid 1,4-hydride ion transfer in *o*-$CH_3OC_6H_4^+$ from the methyl moiety to the vacant ring orbital. The effects of the X substituent upon the behavior of arylium ions in both gaseous and liquid media have been compared with the data of previous related studies and are discussed in light of theoretical predictions.

Introduction

In the last two decades, a number of papers clearly and convincingly demonstrated that arylium ions are key intermediates in the dediazoniation of arenediazonium salts in solution.[1] More recently, increasing interest in these elusive intermediates focused on their structure and spin multiplicity as well as on their reactivity as a function of the nature and the position of substituents in the aromatic ring.[2,3] These questions were first addressed in a pioneering work by Taft[4] who interpreted the anomalous enhancement in the thermal decomposition rate of *m*-methoxybenzenediazonium salts as due to the extensive charge dispersal in the incipient *m*-$CH_3OC_6H_4^+$ ion from its nominally vacant sp^2 orbital to the formally orthogonal π system. This situation, which seems to be accessible only to phenylium ions containing electron releasing groups in the *meta* positions, requires nevertheless a large distortion of the geometry of the ion from planarity,[5] which may promote conceivable intersystem crossing to a triplet ground state or profound structural rearrangements.[6] To date, incidental indications about the substituent effects on the electronic state ordering of arylium ions rest on theoretical calculations[2] and on electron spin resonance (ESR) spectra of arenediazonium salts irradiated at the liquid N_2 temperature.[3] The emerging picture is far from definitive for the following reasons.

On the one hand, theoretical calculations, performed at inadequate levels of theory on nonoptimized struc-

[†] Istituto di Chimica Nucleare del C.N.R.
[‡] Deceased Dec 1993.
[§] Università di Roma "La Sapienza".
[⊗] Abstract published in *Advance ACS Abstracts,* February 1, 1995.

(1) (a) Zollinger, H. *Acc. Chem. Res.* **1974**, *6*, 336. (b) Zollinger, H. *Angew. Chem., Int. Ed. Engl.* **1978**, *17*, 141. (c) Swain, C. G.; Sheats, J. E.; Harbison, K. G. *J. Am. Chem. Soc.* **1975**, *97*, 783. (d) Swain, C. G.; Sheats, J. E.; Gorenstein, D. G.; Harbison, K. G. *Ibid.* 791. (e) Swain, C. G.; Sheats, J. E.; Harbison, K. G. *Ibid.* 796. (f) Broxton, T. J.; Bunnett, J. F.; Paik, C. H. *J. Chem. Soc., Chem. Commun.* **1970**, 1363. (g) Bergstrom, R. G.; Landells, R. G. M.; Wahl, G. H., Jr.; Zollinger, H. *J. Am. Chem. Soc.* **1976**, *98*, 3301. (h) Bunnett, J. F.; Yijima, C. *J. Org. Chem.* **1977**, *42*, 639. (i) Szele, I.; Zollinger, H. *J. Am. Chem. Soc.* **1978**, *100*, 2811. (j) Tröndlin, F.; Medina, R.; Rüchardt, C. *Chem. Ber.* **1979**, *112*, 1835. (k) Scaiano, J. C.; Kim-Thuan, N.; Leigh, W. J. *J. Photochem.* **1984**, *24*, 79.

(2) (a) Evlet, E. M.; Horowitz, P. M. *J. Am. Chem. Soc.* **1971**, *93*, 5636. (b) Gleiter, R.; Hoffmann, R.; Stohrer, W. D. *Chem. Ber.* **1972**, *105*, 8. (c) Dill, J. D.; Schleyer, P. v. R. *Tetrahedron Lett.* **1975**, *33*, 2857. (d) Dill, J. D.; Schleyer, P. v. R.; Pople, J. A. *J. Am. Chem. Soc.* **1977**, *99*, 1. (e) Koser, G. F. *J. Org. Chem.* **1977**, *42*, 1474.

(3) (a) Cox, A.; Kemp, T. J.; Payne, D. R.; Symons, H. C. R.; Pinot de Moira, P. *J. Am. Chem. Soc.* **1978**, *100*, 4779. (b) Ambroz, H. B.; Kemp, T. J. *J. Chem. Soc., Perkin Trans. 2* **1979**, 1420. (c) Ambroz, H. B.; Kemp, T. J. *J. Chem. Soc., Perkin Trans. 2* **1980**, 768. (d) Ambroz, H. B.; Kemp, T. J. *J. Chem. Soc., Chem. Commun.* **1982**, 172. (e) Ambroz, H. B.; Kemp, T. J. *Chem. Soc. Rev.* **1979**, *8*, 353.

(4) Taft, R. W. *J. Am. Chem. Soc.* **1961**, *83*, 3350. See also: (a) Abramovitch, R. A.; Hymers, W. A.; Rajan, J. B.; Wilson, R. *Tetrahedron Lett.* **1963**, *23*, 1507. (b) Abramovitch, R. A.; Terzakian, G. *Can. J. Chem.* **1965**, *43*, 940. (c) Abramovitch, R. A.; Saha, J. G. *Can. J. Chem.* **1965**, *43*, 3269.

(5) (a) Kobayashi, H.; Sonoda, T. Proceedings of the IV Kyushu International Symposium on Physical Organic Chemistry, Fukuoka and Ube, Japan, 1991. (b) Harada, M.; Nakatsuji, T.; Hori, K.; Sonoda, T.; Kobayashi, H. Proceedings of the V Kyushu International Symposium on Physical Organic Chemistry, Fukuoka, Japan, 1993.

(6) (a) Speranza, M. *Tetrahedron Lett.* **1980**, *21*, 1983. (b) Angelini, G.; Fornarini, S.; Speranza, M. *J. Am. Chem. Soc.* **1982**, *104*, 4773. (c) Speranza, M.; Keheyan, Y.; Angelini, G. *J. Am. Chem. Soc.* **1983**, *105*, 6377. (d) Cacace, F.; Ciranni, G.; Sparapani, C.; Speranza, M. *J. Am. Chem. Soc.* **1984**, *106*, 8046. (e) Castenmiller, W. A.; Buck, H. M. *Recl. Trav. Chim.Pays-Bas* **1977**, *96*, 207. (f) Tasaka, M.; Ogata, M.; Ichikawa, H. *J. Am. Chem. Soc.* **1981**, *103*, 1885. (g) Schleyer, P. v. R.; Kos, A. J.; Ragavachari, K. *J. Chem. Soc., Chem. Commun.* **1983**, 1296.

0022-3263/95/1960-1250$09.00/0

tures,[2] predict singlet configuration to be best stabilized in arylium ions substituted by σ-donors (i.e., Li, HBe, H_2B, and H_3C) in the order *ortho* > *meta* > *para*, whereas triplet configuration is best stabilized by π- donors (i.e., H_2N, HO, and F) in the order *para* ≈ *ortho* > *meta*. Accordingly, theory predicts singlet ground states for all arylium ions bearing the above substituents, except for the $H_2NC_6H_4^+$ isomers and for *o*- and *p*- (but not *meta*) $HOC_6H_4^+$ ions. Incidentally, theory did not provide any information about the effects of substituents, such as NO_2 and CN, which are recognized as σ- and π-acceptors and, thus, expected to destabilize both singlet and triplet configurations.

On the other hand, ESR evidence points to triplet ground states only for *m*- and *p*-$R_2NC_6H_4^+$,[3] perhaps as a consequence of the experimental conditions (i.e., effects of matrix, counterion, temperature, etc.) on the stationary concentrations of arylium intermediates in the singlet and triplet configurations.

Finally, the picture becomes even fuzzier by the observation that both theoretical and ESR evidence are inconsistent with Taft's view of a triplet ground state for *m*-$CH_3OC_6H_4^+$.[4]

In the attempt to widen the experimental approach to the problem, it was decided to undertake a comprehensive study of the structure and reactivity properties of isomeric $XC_6H_4^+$ ions by using the method based on β^- decay of ^3H atoms in suitably labeled substituted benzenes. The nuclear decay technique, whose principles and applications have been extensively reviewed,[7] allows generation and investigation of virtually all carbocations, with well-defined structure and free of massive counterions, in any system of interest from diluted gaseous state to condensed phase. Since the decay event generates exactly the same carbocation in any media, the technique represents the tool choice for contrasting the behavior of the same ion in gaseous and liquid phase and for establishing a direct link between gas phase experimental results and theoretical predictions, normally referring to isolated species. In the specific case of arylium ions, the interest is not restricted to comparison purposes, since the technique outlined in this paper could represent a unique tool for the study for these species which is severely hampered, from the theoretical side, by limitation of the basis sets and the computational level and, from the experimental side, by the lack in solution of clean routes to them. Indeed, the decay technique has been successfully applied to gather otherwise unaccessible information on the structure, spin multiplicity, and reactivity of free phenylium[6a,c,8] and tolylium ions.[6d,9] Along the same lines, the study is now extended to $XC_6H_4^+$ ions containing substituents, i.e., X = NO_2, CN, Cl, Br, OH, and OCH_3, with largely different electronic properties.

Experimental Section

Materials. The synthetic sequence adopted to prepare ring-multitritiated substituted benzenes XC_6H_5 (*H* = H or T), precursors of isomeric $XC_6H_4^+$, is shown in Chart 1, together with the absolute and specific activity of the starting C_6H_6[10] and its derivatives and the chemical and radiochemical yields of each synthetic step. Blank runs, carried out using C_6D_6 as starting compound, showed that each step of the sequence involves no more than 2.8% of deuterium exchange distributed almost uniformly on all ring positions of XC_6H_5 (last column of Chart 1). Concerning the tritium content in XC_6H_5, a rough estimate can be derived from best fitting between the experimental and theoretical time dependence of the activity of starting XC_6H_5 and of its neutral labeled products from liquid samples expressed by

$$S_t = S_A \sum_{n=1}^{5} \{\chi_n[\exp(-nkt)]\} \quad (1)$$

$$P_t = \alpha S_A \sum_{n=1}^{5} (n-1)\chi_n \{\exp[-(n-1)kt] - \exp[-nkt]\} \quad (2)$$

where S_A is the initial activity of XC_6H_5, S_t is the residual activity of XC_6H_5 after the decay time t, P_t is the overall activity in the decay products after t, k is the tritium decay rate constant; χ_n is the activity fraction of $XC_6H_{5-n}T_n$, and α is the fraction of the decay ions retaining the arylium ion structure. On these grounds, the χ_n distribution of the XC_6H_5 compounds of Chart 1 is found to peak for an n value ranging between 2 and 3, whereas the structural retention factor α averages around 0.8.

The crude XC_6H_5 products from the synthetic sequence of Chart 1 were purified by preparative GLC, using the following columns: (i) a 5-m long, 4-mm-i.d. column, packed with 15% OS550 on 80/100 mesh Chromosorb WHP, operated at 100–200 °C; (ii) a 5-m long, 4-mm-i.d. column, packed with 10% Apiezon L on 80/100 mesh Chromosorb WHP, operated at 150–200 °C; (iii) a 2.5-m long, 4-mm-i.d. column, packed with Porapak Q, operated at 100–200 °C.

Methanol and the aromatic compounds used as carriers or as standards in the GLC analysis were research grade chemicals from Aldrich Co. and were used without further purification. Ucar Co. provided O_2, $(CH_3)_3N$, and methyl halides CH_3Y (Y = F, Cl, and Br), with a stated purity exceeding 99.0 mol %.

Growth of the Decay Products. The procedures followed to prepare the gaseous and liquid samples were analogous to those described elsewhere.[6b]

The gaseous samples were prepared by introducing ca. 0.3–1.0 mCi of purified XC_6H_5 into carefully evacuated and outgassed 500-mL Pyrex vessels containing measured amounts of CH_3OH or CH_3Y (Y = F, Cl, or Br) together with O_2 (4 Torr), used as a radical scavenger, and the base $(CH_3)_3N$ (10 Torr), when required. Therefore, the vessels were sealed off and stored in the dark, at room temperature, for 12–16 months.

The liquid systems were prepared by mixing ca. 0.1–0.3 mCi of purified XC_6H_5 into a 2 mL of CH_3OH. The mixture was then introduced into a 2.5-mL ampule, connected through a long, narrow arm to a vacuum line. After the mixture was frozen with a liquid N_2 bath, the ampule was evacuated and eventually sealed off. The vials were stored in the dark at room temperature for periods ranging from 12 to 16 months.

Analysis of the Decay Products. A Model Beckman (System Gold) radio-HPLC chromatograph, equipped with a variable-wavelength UV detector in series to a Berthold flow-scintillation counter, was used for chromatographic analysis

(7) For recent reviews, see: (a) Speranza, M. *Chem. Rev.* **1993**, *93*, 2933. (b) Cacace, F. *Science* **1990**, *250*, 392. (c) Cacace, F.; Speranza, M. In *Techniques for the Study of Ion/Molecule Reactions*; Farrar, J. M., Saunders, W. H., Jr., Eds.; Wiley: New York, 1988; Chapter VI.

(8) (a) Angelini, G.; Sparapani, C.; Speranza, M. *Tetrahedron* **1984**, *40*, 4865. (b) Fornarini, S.; Speranza, M. *J. Chem. Soc., Chem. Commun.* **1985**, 1692. (c) Fornarini, S.; Speranza, M. *J. Am. Chem. Soc.* **1985**, *107*, 5358. (d) Colosimo, M.; Speranza, M.; Cacace, F.; Ciranni, G. *Tetrahedron* **1984**, *40*, 4873. (e) Fornarini, S.; Speranza, M. *Gazz. Chim. Ital.* **1986**, *116*, 341. (f) Angelini, G.; Keheyan, Y.; Speranza, M. *Helv. Chim. Acta* **1988**, *71*, 107. (g) Filippi, A.; Occhiucci, G.; Speranza, M. *Can. J. Chem.* **1991**, *69*, 732. (h) Keheyan, Y.; Speranza, M. *Helv. Chim. Acta* **1985**, *68*, 2381. (i) Fornarini, S.; Speranza, M. *J. Chem. Soc., Perkin Trans. 2* **1984**, 171. (j) Fornarini, S.; Speranza, M. *Can. J. Chem.* **1988**, *66*, 2506.

(9) Angelini, G.; Sparapani, C.; Speranza, M. *J. Chem. Soc., Perkin Trans. 2* **1988**, 1393.

(10) Cacace, F.; Speranza, M.; Wolf, A. P.; Ehrenkaufer, R. *J. Labelled Compds Radiopharm.* **1982**, *19*, 905.

Chart 1

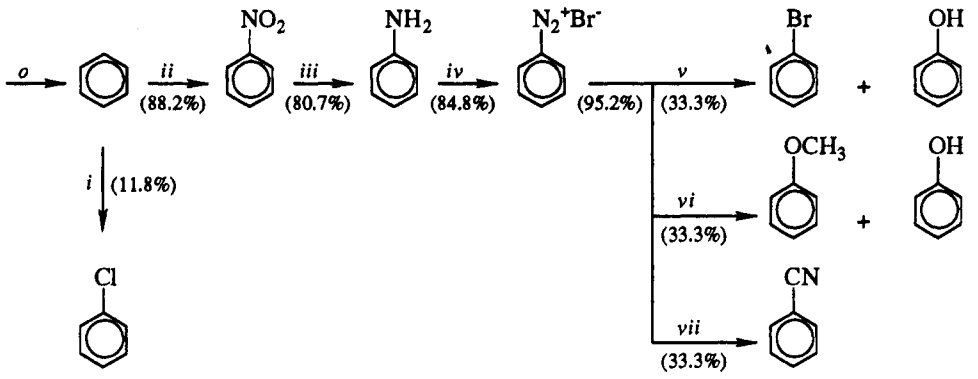

i) $TiCl_4$, CF_3CO_3H, CH_2Cl_2, 20 °C ; *ii)* HNO_3/H_2SO_4, 0 °C; *iii)* N_2H_4, Ni - Raney, 110 °C; *iv)* HBr, $NaNO_2$, 0 °C; *v)* $CuSO_4 \cdot 5H_2O$, NaBr, Na_2SO_3, 0 °C; *vi)* CH_3OH, 0 °C; *vii)* $CuSO_4 \cdot 5H_2O$, NaCN, Na_2SO_3, 0 °C.
The figures in parentheses refer to the fraction of reactant used in the corresponding synthetic step. The remainders were used in the decay experiments.

Substituent (X)	Step	Total Activity (Ci)	Specific Activity (Ci mol^{-1})	Chemical Yield (%)	Radiochemical Yield (%)	Total Isotopic Exchange (%)
H	*o*	2.055	53.6			
Cl	*i*	0.106	43.4	54.0	52.5	2.8
NO_2	*ii*	1.114	43.9	75.0	73.8	1.6
NH_2	*iii*	0.836	43.0	95.0	93.0	2.1
$N_2^+Br^-$	*iv*	0.744	42.9	91.2	89.0	0.1
Br	*v*	0.162	42.9	69.0	68.7	0.4
OCH_3	*vi*	0.087	42.8	37.0	36.8	0.6
OH	*v* + *vi*	0.100	42.6	21.3	21.2	1.1
CN	*vii*	0.128	42.5	55.0	54.5	0.9

of the decay mixtures. After the storage time, the vessels containing the gaseous mixtures were cooled at the liquid N_2 temperature and opened and their contents washed with ca. 0.5 mL of CH_3OH. The liquid solutions were directly subjected to radio-HPLC analyses. The identity of the radioactive products was established by comparing their retention volumes with those of authentic samples on the following columns: (i) a 25-cm long, 4.6-mm-i.d. column, packed with 5-μm Supelco Ultrasphere ODS; (ii) a 25-cm long, 4.6-mm-i.d. column, packed with 5-μm Supelco Supelcosil LC-8; (iii) a 20-cm long, 4.6-mm-i.d. column, packed with 5-μm Chromsep Hypersil ODS; (iv) a 25-cm long, 4.6-mm-i.d. column, packed with 5-μm Supelco Supelcosil LC-18; (v) a 20-cm long, 4.6-mm-i.d. column, packed with 5-μm Chromsep Chromspher C-8. Sometimes, the H_2O/CH_3OH or C_2H_5OH eluent mixture was added with 3.5–16 mM aqueous solutions of β-cyclodextrin.

The absolute yield of the labeled aromatic products was deduced from the ratio of their overall activity to the total activity of the $XC_6H_4^+$ decay ions, expressed by eq 2. The overall activity of the decay aromatic products is in turn calculated from the ratio of their combined peak areas to that of the starting XC_6H_5 compound, multiplied by the residual activity of the latter as derived from eq 1.

Computational Details. *Ab initio* calculations have been performed using a RISC/6000 version of the GAUSSIAN 92 set of programs.[11] The 6-31 G*[12] basis set was employed to optimize the geometries of the investigated species at the Hartree–Fock level of theory (HF), as well as to obtain the corresponding vibrational frequencies. Single-point calculations, at the Møller-Plesset[13] second-order level of theory (MP2), were performed at the HF/6-31G*-optimized geometries in order to include the correlation energy effects on the relative stability of the investigated species.

Results

Table 1 reports the absolute and relative yields of the labeled aromatic products from the attack of isomeric $O_2NC_6H_4^+$ ions on CH_3OH and CH_3Cl and the composition of the corresponding decay systems. The results concerning the reactions of $NCC_6H_4^+$ on CH_3OH and CH_3Y (Y = F, Cl, and Br) are listed in Table 2.

Tables 3–6 report the absolute and relative yields of the tritiated aromatic derivatives of $XC_6H_4^+$ (X = Cl, Br, OH and OCH_3) when generated by nuclear decay of XC_6H_5 in gaseous and liquid CH_3OH and in gaseous CH_3Y (Y = Cl, Br) at room temperature.

The overall absolute yields of the products of Tables 1–4 and 6 recovered in liquid CH_3OH account for 68–87% of the activity contained in their nucleogenic precursors $XC_6H_4^+$ (X = NO_2, CN, Cl, Br, and OCH_3). Appreciably lower are instead the absolute yields of the products from $HOC_6H_4^+$ (48%) (Table 5) in the same medium. The overall absolute yields of the products from the gaseous samples approach those measured in liquid CH_3OH and tend to decrease by lowering the system pressure. Such a decrease is partly counterbalanced by formation of low-boiling fragmentation products and

(11) GAUSSIAN 92, Revision A: Frish, M. J.; Trucks, G. W.; Head-Gordon, M.; Gill, P. M. W.; Wong, M. W.; Foresman, J. B.; Johnson, B. G.; Schlegel, H. B.; Robb, M. A.; Replogle, E. S.; Gomperts, R.; Andres, J. L.; Ragavachari, K.; Binkley, J. S.; Gonzalez, C.; Martin, R. L.; Fox, D. J.; Defrees, D. J.; Baker, J.; Stewart, J. J. P.; Pople, J. A. Gaussian, Inc., Pittsburgh, PA 1992.

(12) Hariharan, P. C.; Pople, J. A. *Chem. Phys. Lett.* **1972**, *66*, 217.

(13) Møller, C.; Plesset, M. S. *Phys. Rev.* **1934**, *46*, 86.

Table 1. Radioactive Products form the Decay of $O_2NC_6H_5$ in CH_3OH and CH_3Cl

system composition[a]		product distribution,[b] %									
		$O_2NC_6H_4OCH_3$			$O_2NC_6H_4OH$			$O_2NC_6H_4CH_2OH$			total
CH_3OH (Torr)	$O_2NC_6H_5$ (mol %)	*ortho*	*meta*	*para*	*ortho*	*meta*	*para*	*ortho*	*meta*	*para*	absolute yield, %
liquid	0.014	20 (0.8)	49 (2.0)	25 (1.0)	nd (−)[c]	2 (2.0)	1 (1.0)	nd (−)	1 (0.5)	2 (1.0)	68
gas (65)	0.98	nd (−)	35 (2.1)	17 (1.0)	nd (−)	25 (1.9)	13 (1.0)	2 (0.7)	4 (1.3)	3 (1.0)	56
gas (50)	1.06	nd (−)	29 (2.6)	11 (1.0)	nd (−)	31 (1.7)	18 (1.0)	2 (0.5)	5 (1.2)	4 (1.0)	52
gas (20)	2.39	nd (−)	21 (2.1)	10 (1.0)	nd (−)	40 (2.9)	14 (1.0)	4 (0.8)	6 (1.2)	5 (1.0)	51

		$O_2NC_6H_4Cl$			
CH_3Cl (Torr)		*ortho*	*meta*	*para*	
gas (760)	0.09	nd (−)	71 (2.4)	29 (1.0)	89
gas (200)	0.30	nd (−)	69 (2.2)	31 (1.0)	71
gas (100)	0.78	nd (−)	65 (1.9)	35 (1.0)	70
gas (50)	1.55	nd (−)	67 (2.0)	33 (1.0)	72
gas (40)	1.54	nd (−)	70 (2.3)	30 (1.0)	53
gas (30)	2.36	nd (−)	71 (2.4)	29 (1.0)	44
gas (20)	3.35	nd (−)	69 (2.2)	31 (1.0)	51
gas (10)	7.63	nd (−)	65 (1.9)	35 (1.0)	52

[a] 4 Torr of O_2, present in the gaseous samples as a radical scavenger; $O_2NC_6H_5$ activity: 0.2−0.6 mCi. [b] The figures in parentheses refer to the *ortho*:*meta*:*para* ratios. [c] nd = below detection limit: ca. 0.5%.

Table 2. Radioactive Products form the Decay of NCC_6H_5 in CH_3OH and CH_3Y (Y = F, Cl, and Br)

system composition[a]		product distribution,[b] % $NCC_6H_4OCH_3$			total
CH_3OH (Torr)	NCC_6H_5 (mol %)	*ortho*	*meta*	*para*	absolute yield, %
liquid	0.016	34 (1.5)	43 (1.9)	23 (1.0)	79
gas (65)	1.17	32 (1.6)	48 (2.4)	20 (1.0)	55
gas (30)	2.68	30 (1.3)	47 (2.0)	23 (1.0)	48
gas (10)	7.37	37 (2.0)	45 (2.5)	18 (1.0)	44
gas (5)	14.88	38 (2.0)	43 (2.3)	19 (1.0)	45

		NCC_6H_4Y			$CH_3NHCOC_6H_4Y$			
CH_3Br (Torr)		*ortho*	*meta*	*para*	*ortho*	*meta*	*para*	
gas (760)	0.06[c]	36 (1.7)	43 (2.0)	21 (1.0)				52
gas (760)	0.08	34 (1.5)	43 (1.9)	23 (1.0)				59
gas (200)	0.31	33 (1.4)	44 (1.9)	23 (1.0)				51
gas (40)	1.59	38 (1.7)	40 (1.8)	22 (1.0)				43
gas (20)	3.09	38 (1.6)	39 (1.7)	23 (1.0)				42
CH_3Cl (Torr)								
gas (100)	0.70	26 (2.2)	47 (3.9)	12 (1.0)	10 (1.2)	nd (−)[d]	8 (1.0)	49
gas (40)	1.74	17 (5.7)	50 (16.7)	3 (1.0)	27 (1.7)	nd (−)	16 (1.0)	45
gas (20)	2.98	15 (2.5)	42 (7.0)	6 (1.0)	28 (3.1)	nd (−)	9 (1.0)	41
gas (10)	6.74	17 (3.4)	56 (11.2)	5 (1.0)	15 (2.5)	nd (−)	6 (1.0)	36
CH_3F (Torr)								
gas (200)	0.30	1 (0.03)	48 (1.4)	33 (1.0)	18 (−)	nd (−)	nd (−)	46

[a] 4 Torr of O_2, present in the gaseous samples as a radical scavenger; NCC_6H_5 activity: 0.2−0.7 mCi. [b] The figures in parentheses refer to the *ortho*:*meta*:*para* ratios. [c] $(CH_3)_3N$: 10 Torr. [d] nd = below detection limit: ca. 0.5%.

high-boiling aromatic oligomers, presumably arising from direct attack of the nucleogenic ions, or their fragments, on the aromatic substrate itself. The remainder is provided by the formation of XC_6H_4H products, whose activity cannot be discriminated from that contained in the undecayed starting compounds.

The results of Table 1 most relevant to the specific purposes of this study can be itemized as follows: (i) In liquid CH_3OH, nitroanisoles are by far the predominant products (94%), accompanied by minor yields of nitrophenols (3%), and nitrobenzyl alcohols (3%). The isomeric composition of nitroanisoles (*ortho*, 21%; *meta*, 52%; *para*, 27%) does not match that of their $O_2NC_6H_4^+$ precursors (*ortho*, 40%; *meta*, 40%; *para*, 20%), expected on the grounds of the $O_2NC_6H_5$ synthetic procedure (Chart 1) and the results of the blank runs with C_6D_6 as the starting compound.[14] In fact, while the *meta*:*para* = 2:1 ratio of $O_2NC_6H_4^+$ is maintained in $O_2NC_6H_4OCH_3$, the proportion of the *ortho* isomer is less than half of that expected. The isomeric composition of nitrophenols parallels that of nitroanisoles, with the yield of the *ortho* isomer below the detection limit (ca. 0.5%). (ii) In gaseous CH_3OH, much higher yields of nitrophenols (38−54%) and nitrobenzyl alcohols (9−15%) accompany formation of nitroanisoles. While the *ortho* isomer is detectable in nitrobenzyl alcohols, it is undetectable not only in nitrophenols, but also in nitroanisoles. In both these classes of products, the *meta*:*para* distribution stays fairly close to the 2:1 ratio measured in liquid CH_3OH. (iii) In gaseous CH_3Cl the $O_2NC_6H_4Cl$ distribution reflects that of $O_2NC_6H_4OR$ (R = H, CH_3) observed in gaseous CH_3OH, characterized by the absence of the *ortho* isomer and by a *meta*:*para* ratio close to 2.

The results of Table 2 can be summarized as follows: (i) in both liquid and gaseous CH_3OH as well as in CH_3-

(14) An additional check of the *ortho*:*meta*:*para* = 2:2:1 distribution of tritium atoms in $O_2NC_6H_5$ is provided by the observation that many of its XC_6H_5 derivatives of Chart 1, when decaying in liquid CH_3OH, give rise to labeled products with an isomeric distribution close to *ortho*:*meta*:*para* = 2:2:1 (see, for instance, Table 2).

Table 3. Radioactive Products from the Decay of ClC_6H_5 in CH_3OH and CH_3Y (Y = Cl, Br)

system composition[a]		product distribution,[b] %						total absolute yield, %
		$ClC_6H_4OCH_3$			ClC_6H_4OH			
CH_3OH (Torr)	ClC_6H_5 (mol %)	*ortho*	*meta*	*para*	*ortho*	*meta*	*para*	
liquid	0.005	35 (1.7)	44 (2.1)	21 (1.0)	nd[c]	nd	nd	86
gas (65)	0.79[d]	34 (1.6)	45 (2.1)	21 (1.0)	nd	nd	nd	52
gas (65)	0.97	30 (1.9)	36 (2.2)	16 (1.0)	8 (1.3)	5 (0.8)	6 (1.0)	63
gas (5)	13.54	19 (1.6)	35 (2.9)	12 (1.0)	21 (3.5)	7 (1.2)	6 (1.0)	50
		ClC_6H_4Y						
CH_3Cl (Torr)		*ortho*		*meta*		*para*		
gas (760)	0.11[d]	36 (1.8)		44 (2.2)		20 (1.0)		60
gas (760)	0.09	39 (1.9)		41 (2.0)		20 (1.0)		66
gas (200)	0.34	38 (1.8)		41 (1.9)		21 (1.0)		70
gas (100)	0.82	39 (1.9)		41 (2.0)		20 (1.0)		68
gas (30)	2.37	38 (1.8)		41 (1.9)		21 (1.0)		63
gas (10)	7.00	38 (1.8)		41 (1.9)		21 (1.0)		65
CH_3Br (Torr)								
gas (760)	0.06[e]	39 (1.9)		41 (2.0)		20 (1.0)		66
gas (760)	0.06[d]	39 (2.0)		42 (2.2)		19 (1.0)		66
gas (760)	0.06	39 (1.9)		41 (2.0)		20 (1.0)		78
gas (200)	0.21	39 (1.9)		41 (2.0)		20 (1.0)		70
gas (100)	0.53	38 (1.9)		42 (2.1)		20 (1.0)		63
gas (40)	1.37	38 (1.9)		42 (2.1)		20 (1.0)		58
gas (20)	2.04	37 (1.8)		43 (2.1)		20 (1.0)		52
gas (10)	6.06	36 (1.7)		43 (2.0)		21 (1.0)		52

[a] 4 Torr of O_2, present in the gaseous samples as a radical scavenger; ClC_6H_5 activity: 0.1–0.9 mCi. [b] The figures in parentheses refer to the *ortho*:*meta*:*para* ratios. [c] nd = below detection limit: ca. 0.5%. [d] $(CH_3)_3N$: 10 Torr. [e] $(CH_3)_3N$: 20 Torr.

Table 4. Radioactive Products from the Decay of BrC_6H_5 in CH_3OH and CH_3Y (Y = Cl, Br)

system composition[a]		product distribution,[b] %						total absolute yield, %
		$BrC_6H_4OCH_3$			BrC_6H_4OH			
CH_3OH (Torr)	BrC_6H_5 (mol %)	*ortho*	*meta*	*para*	*ortho*	*meta*	*para*	
liquid	0.012	37 (1.8)	42 (2.0)	21 (1.0)	nd[c]	nd	nd	87
gas (65)	0.96[d]	34 (1.7)	46 (2.3)	20 (1.0)	nd	nd	nd	53
gas (65)	0.90	19 (1.7)	32 (2.9)	11 (1.0)	17 (1.9)	12 (1.3)	9 (1.0)	67
gas (30)	1.90	17 (1.7)	31 (3.1)	10 (1.0)	19 (1.9)	13 (1.3)	10 (1.0)	62
gas (10)	7.34	20 (1.7)	36 (3.0)	12 (1.0)	17 (2.1)	7 (0.9)	8 (1.0)	57
gas (5)	11.53	21 (1.7)	37 (3.1)	12 (1.0)	16 (2.3)	7 (1.0)	7 (1.0)	57
		BrC_6H_4Y						
CH_3Cl (Torr)		*ortho*		*meta*		*para*		
gas (760)	0.09[d]	38 (2.0)		43 (2.3)		19 (1.0)		66
gas (760)	0.10	39 (1.9)		41 (2.0)		20 (1.0)		72
gas (200)	0.37	38 (1.9)		42 (2.1)		20 (1.0)		69
gas (100)	0.75	39 (1.9)		41 (2.0)		20 (1.0)		69
gas (50)	1.47	39 (2.0)		42 (2.2)		19 (1.0)		66
gas (30)	2.41	35 (1.5)		42 (1.8)		23 (1.0)		64
gas (20)	3.56	38 (1.9)		42 (2.1)		20 (1.0)		62
gas (10)	13.85	37 (1.7)		41 (1.9)		22 (1.0)		62
CH_3Br (Torr)								
gas (760)	0.07[d]	39 (1.9)		41 (2.0)		20 (1.0)		67
gas (760)	0.08	40 (2.0)		40 (2.0)		20 (1.0)		74
gas (100)	0.55	34 (1.5)		44 (2.0)		22 (1.0)		57

[a] 4 Torr of O_2, present in the gaseous samples as a radical scavenger; BrC_6H_5 activity: 0.2–0.9 mCi. [b] The figures in parentheses refer to the *ortho*:*meta*:*para* ratios. [c] nd = below detection limit: ca. 0.5%. [d] $(CH_3)_3N$: 10 Torr.

Br, the only recovered derivatives of $NCC_6H_4^+$ are, respectively, the isomeric methoxybenzonitriles and bromobenzonitriles, in proportions approaching those of their ionic precursors (*ortho*, 40%; *meta*, 40%; *para*, 20%); (ii) in gaseous CH_3F, the isomeric distribution of fluorobenzonitrile products is characterized by the substantial depletion of the *ortho* isomer, which is counterbalanced in part by the formation of significant amounts of *o*-*N*-methyl fluorobenzamide; (iii) in gaseous CH_3Cl as well, the isomeric distribution of chlorobenzonitrile products is characterized by formation of the *ortho* and *para* isomers in proportions well below those of the corresponding $NCC_6H_4^+$ precursors. The unbalance is mostly relieved by considering the accompanying formation of *o*- and *p*-*N*-methylchlorobenzamides. In fact, when the yields of the *ortho* and *para* isomers of both classes of products are combined, an *ortho*:*meta*:*para* distribution is obtained which closely parallels that of $NCC_6H_4^+$ (*ortho*:*meta*:*para* = 2:2:1), especially at the highest CH_3Cl pressures (*ortho*:*meta*:*para* = 1.8:2.3:1.0).

The results of Tables 3 and 4 can be summarized as follows: (i) in liquid CH_3OH, haloanisoles are exclusively formed, whose isomeric distributions approximately reflect those of the $XC_6H_4^+$ (X = Cl, Br) precursors (*ortho*,

Table 5. Radioactive Products from the Decay of HOC_6H_5 in CH_3OH and CH_3Cl

system composition[a]		product distribution,[b] % $HOC_6H_4OCH_3$			total absolute yield, %
CH_3OH (Torr)	HOC_6H_5 (mol %)	*ortho*	*meta*	*para*	
liquid	0.014	5 (0.2)	69 (2.6)	26 (1.0)	48
gas (65)	0.98	38 (0.6)	3 (0.05)	59 (1.0)	27
gas (5)	9.66	50 (1.1)	4 (0.09)	46 (1.0)	25
		HOC_6H_4Cl			
CH_3Cl (Torr)		*ortho*	*meta*	*para*	
gas (760)	0.04	41 (2.0)	39 (1.9)	20 (1.0)	52
gas (200)	0.29	43 (2.5)	40 (2.3)	17 (1.0)	50
gas (100)	0.69	37 (1.8)	43 (2.1)	20 (1.0)	47
gas (40)	1.71	35 (1.3)	39 (1.5)	26 (1.0)	46
gas (20)	3.57	31 (1.1)	41 (1.5)	28 (1.0)	44
gas (10)	6.21	31 (1.0)	39 (1.3)	30 (1.0)	40

[a] 4 Torr of O_2, present in the gaseous samples as a radical scavenger; HOC_6H_5 activity: 0.3–0.8 mCi. [b] The figures in parentheses refer to the *ortho*:*meta*:*para* ratios.

Table 6. Radioactive Products from the Decay of $CH_3OC_6H_5$ in CH_3OH and CH_3Cl

		product distribution,[b] %				
system composition[a]		$CH_3OC_6H_4OCH_3$				total
CH_3OH (Torr)	$CH_3OC_6H_5$ (mol %)	*ortho*	*meta*	*para*	C_6H_5OH	absolute yield, %
liquid	0.007	35 (1.7)	45 (2.2)	20 (1.0)	nd[c]	68
gas (65)	0.43	5 (0.2)	64 (2.6)	25 (1.0)	6	40
gas (20)	1.53	1 (0.05)	45 (2.2)	20 (1.0)	34	35
		$CH_3OC_6H_4Cl$				
CH_3Cl (Torr)		*ortho*	*meta*	*para*	C_6H_5Cl	
gas (760)	0.06	7 (0.2)	59 (2.0)	29 (1.0)	5	54
gas (200)	0.22	3 (0.1)	64 (2.4)	27 (1.0)	6	44
gas (50)	0.75	1 (0.04)	61 (2.3)	26 (1.0)	12	47
gas (30)	0.80	1 (0.04)	60 (2.2)	27 (1.0)	11	37

[a] 4 Torr of O_2, present in the gaseous samples as a radical scavenger; $CH_3OC_6H_5$ activity: 0.2–0.5 mCi. [b] The figures in parentheses refer to the *ortho*:*meta*:*para* ratios. [c] nd = below detection limit: ca. 0.5%.

40%; *meta*, 40%; *para*, 20%); (ii) the same picture emerges from the gaseous CH_3OH samples containing 10 Torr of $(CH_3)_3N$. In gaseous CH_3OH without added $(CH_3)_3N$, formation of haloanisoles is accompanied by minor amounts of the corresponding halophenols. While the individual isomeric composition of the two sets of products diverges from that of the $XC_6H_4^+$ precursors, their combined relative yields closely approach the *ortho*:*meta*:*para* = 2:2:1 ratio of initial $XC_6H_4^+$; (iii) in gaseous methyl chloride, the XC_6H_4Cl (X = Cl, Br) distribution matches that of the $XC_6H_4OCH_3$ observed in liquid and gaseous CH_3OH (65 Torr; 10 Torr of $(CH_3)_3N$). The same picture extends to the gaseous methyl bromide samples as well.

The results of Table 5 can be itemized as follows: (i) The only labeled derivatives of $HOC_6H_4^+$, isolated in both liquid and gaseous CH_3OH as well as in CH_3Cl, are the isomeric methoxy and chlorophenols, whose absolute yields depend dramatically upon the nature and the physical state of the nucleophilic acceptor. Thus, the overall yields of methoxyphenols are invariably much lower than those of chlorophenols from the corresponding decay systems. (ii) In liquid CH_3OH, the isomeric composition of methoxyphenols (*ortho*, 5%; *meta*, 69%; *para*, 26%) is characterized by a substantial depletion of the *ortho* isomer relative to the isomeric distribution of the $HOC_6H_4^+$ precursors (*ortho*, 40%; *meta*, 40%; *para*, 20%). (iii) In gaseous CH_3OH, both the absolute yield of methoxyphenols and their isomeric distribution diverge substantially from those observed in liquid CH_3OH. In particular, the methoxyphenol composition is characterized by comparatively low amounts of the *meta* isomer (3–4%) and by an *ortho*:*para* ratio (0.6–1.1) largely diverging from that of initial $HOC_6H_4^+$ ions (*ortho*:*para* = 2). (iv) The *ortho*:*meta*:*para* = 2:2:1 ratio of $HOC_6H_4^+$ precursors is instead reproduced approximately in the chlorophenols recovered from the CH_3Cl samples at the highest pressures (>100 Torr). Below this pressure limit, the isomeric chlorophenol distribution shows a substantial increase of the *para* isomer at the expense of the *ortho* and *meta* ones.

The results of Table 6 can be listed as follows: (i) In liquid CH_3OH, dimethoxybenzenes are the only labeled products, whose isomeric composition parallels that of their ionic precursors $CH_3OC_6H_4^+$ (*ortho*, 40%; *meta*, 40%; *para*, 20%). (ii) The absolute yields of isomeric dimethoxybenzenes from gaseous CH_3OH drops significantly (25–38%), their formation being accompanied by labeled phenol, in relative amounts increasing by decreasing the CH_3OH pressure. Contextually, the isomeric distribution of dimethoxybenzenes changes dramatically as a consequence of the almost complete disappearance of the *ortho* isomer. (iii) A similar picture emerges from the CH_3Cl samples, where predominant formation of chloroanisoles is flanked by minor amounts of chlorobenzene. Under all conditions, the *m*-$CH_3OC_6H_4Cl$:*p*-$CH_3OC_6H_4Cl$ ratio maintains close to 2, namely to the ratio of their initial $CH_3OC_6H_4^+$ precursors, whereas the yield of the *ortho* isomer is comparatively low amounting to values which decrease by decreasing the CH_3Cl partial pressure.

Figures 1 and 2 summarize the results of *ab initio* calculations on isomeric $O_2NC_6H_4^+$ and $HOC_6H_4^+$ ions. For $O_2NC_6H_4^+$, three stationary points corresponding to their ground state geometries **A-C** were located first at HF/6-31G*. These were characterized by vibrational frequency analysis. Single-point calculations at the MP2/

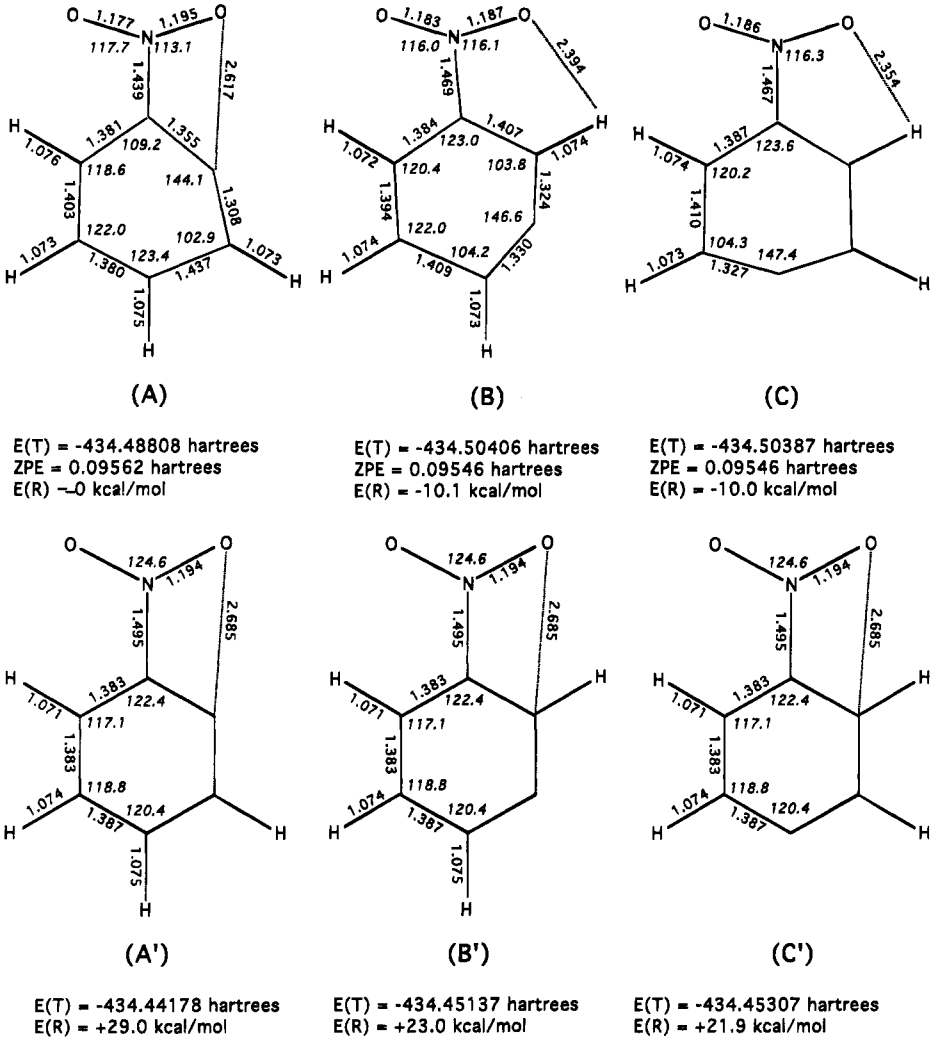

Figure 1. MP2 (FULL)/6-31G*//HF/6-31G* absolute (hartrees) (E(T)) and relative energies (kcal mol^{-1}) (E(R)) and HF/6-31G* ZPE (hartrees) of the HF/6-31G*-optimized structures of relaxed (**A-C**) and nucleogenic (**A'-C'**) nitrophenylium ions. Bond lengths in angstroms and bond angles in degrees (italic).

6-31G*//6-31G* level of theory provided the relative energies reported in Figure 1, which points to a *para* ≈ *meta* > *ortho* stability order for isomeric $O_2NC_6H_4^+$ ions. Single-point calculations at the MP2 level were carried out for isomeric $O_2NC_6H_4^+$ at the geometry of their nitrobenzene precursor (structures **A'**−**C'**). The difference between their total energies and those of the corresponding relaxed structures **A**−**C** allows estimate of the excess vibrational energy in nucleogenic $O_2NC_6H_4^+$ ions, which may amount to ca. 30 kcal mol^{-1}. By the same procedure, a *meta* > *para* > *ortho* stability order was found for isomeric $HOC_6H_4^+$ ions (Figure 2). Again, the energy difference between isomeric $HOC_6H_4^+$ at the geometry of their phenol precursor (structure **D'**−**F'**) and the corresponding relaxed structure **D**−**F** points to an excess vibrational energy in nucleogenic $HOC_6H_4^+$ ions amounting to ca. 33 kcal mol^{-1}.

Discussion

The Reagents. Since the molar fraction of labeled XC_6H_5 (X = NO_2, CN, Cl, Br, OH, and OCH_3) has deliberately been kept at very low levels (<0.0001) in all systems,[15] the otherwise conceivable contribution of radiolytic processes to the formation of tritiated products is practically suppressed.[7] Consequently, in these studies, the labeled decay ions represent the only significant source of the isolated products.

No direct information on the unimolecular, decay-induced fragmentation pattern of tritiated XC_6H_5 is currently available. Nevertheless, theoretical, mass spectrometric, and radiochemical evidence concerning strictly related arenes, such as tritiated benzene and toluene,[9,16] coupled with best fitting evaluation of the α term in eq 2, allow one to delineate with reasonable confidence the molecular consequences of the nuclear decay in XC_6H_5.

The nuclear event is expected to generate in a time (ca. 10^{-15} s) very short on the chemical scale the primary ionic transient $[XC_6H_4{}^3He]^+$ of eq 3.

(15) The molar fraction of labeled XC_6H_5 has been estimated by calculating the mols of XC_6H_5 from the following equation

$$\text{mols of } XC_6H_5 = \sum_{n=1}^{5} \frac{\chi_n(C_i \text{ of } XC_6H_5)}{26\,000n}$$

where the denominator of the fraction refers to the specific activity of *carrier-free* $X_6H_{5-n}T_n$ for any given n value (ref 7c).

(16) (a) Wexler, S. In *Actions Chimiques et Biologiques des Radiations*; Masson, C., Ed.; Huitième Série; Paris: 1965. (b) Ikuta, S.; Okuno, K.; Yashihara, T.; Shiokawa, T. *Radiochem. Radioanal. Lett.* **1975**, *23*, 213. (c) Okuno, K.; Yoshikara, K.; Shiokawa, T. *Radiochim. Acta* **1978**, *25*, 21. (d) Carlson, T. A. *J. Chem. Phys.* **1960**, *32*, 1234. (e) Wexler, S.; Anderson, G. R.; Singer, L. A. *J. Chem. Phys.* **1960**, *32*, 417.

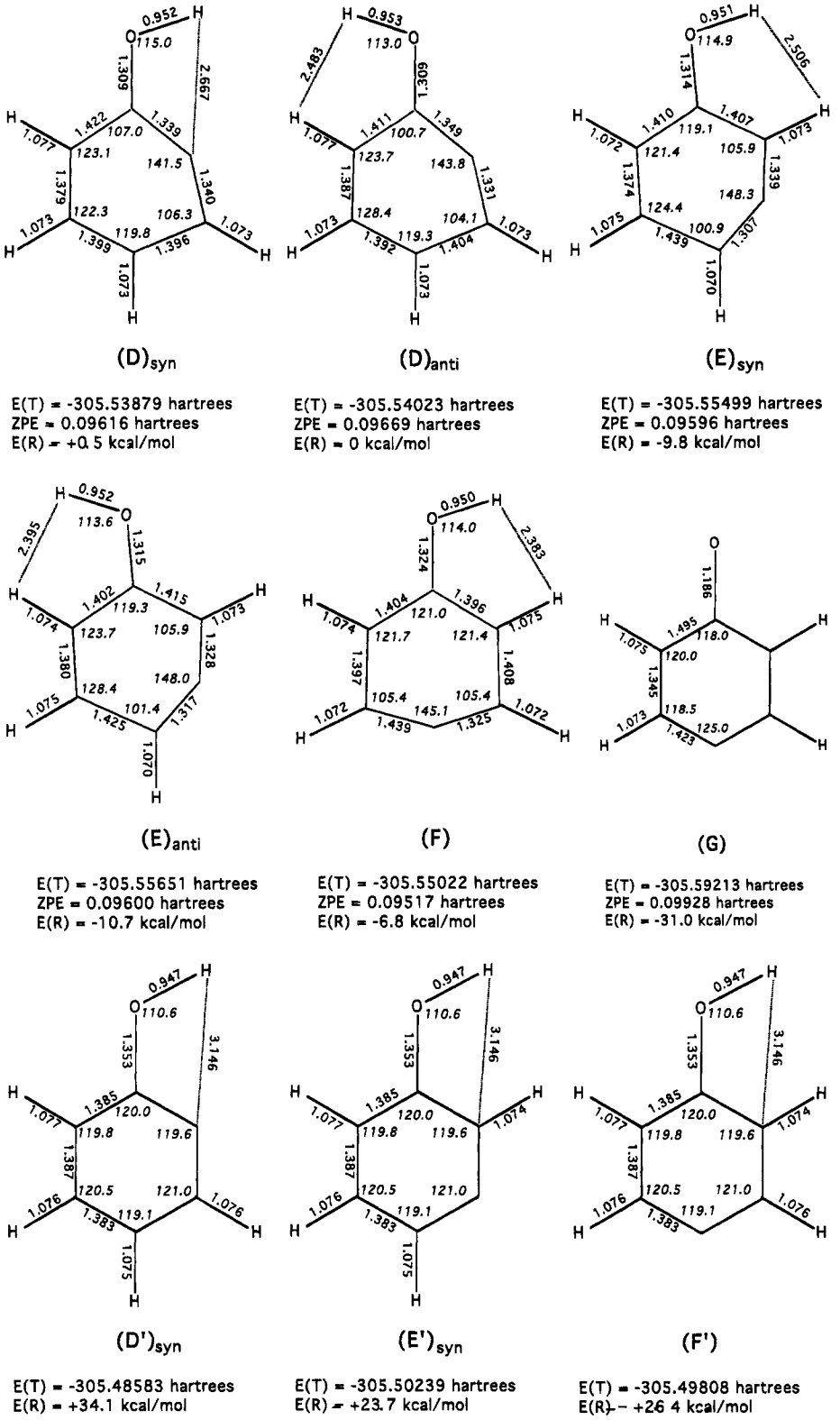

Figure 2. MP2 (FULL)/6-31G*//HF/6-31G* absolute (hartrees) (E(T)) and relative energies (kcal mol^{-1}) (E(R)) and 6-31G* ZPE (hartrees) concerning HF/6-31G*-optimized geometries of relaxed **(D-G)** and nucleogenic **(D'- F')** $[C_6, H_5, O]^+$ ions. Bond lengths in angstroms and bond angles in degrees (italic).

$$XC_6H_5 \xrightarrow{\beta \text{ decay}} [XC_6H_4{}^3He]^+ + \beta^- + \bar{\nu} \qquad (3)$$

According to the unique distribution of excitation energy following tritium decay, well documented by theoretical and mass spectrometric results,[16] up to ca. 20% of the primary $[XC_6H_4{}^3He]^+$ ions are formed in excited electronic states and undergo extensive fragmentation, irrespective of the environment. The remaining major fraction of $[XC_6H_4{}^3He]^+$ ions is formed in their singlet ground state without appreciable recoil energy. Owing to the inherently repulsive nature of the C–He interaction,[17] singlet $[XC_6H_4{}^3He]^+$ ions undergo fast,

(17) Ikuda, S.; Iwata, S.; Imamura, M. *J. Chem. Phys.* **1977**, *66*, 4671.

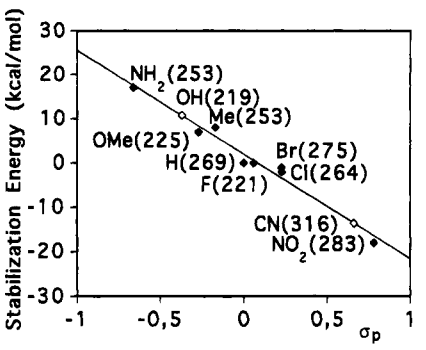

Figure 3. Correlation between the stabilization energy of p-$XC_6H_4^+$, as defined in eq 5, and the σ_p constants of substituents X. The figures in parentheses refer to the heats of formation of p-$XC_6H_4^+$, taken from the literature (ref 19 and Leung, H. W.; Harrison, A. G. *J. Am. Chem. Soc.* **1979**, *101*, 3168) or estimated from the correlation (X = OH and CN).

quantitative loss of the ^{3}He atom yielding singlet $XC_6H_4^+$ and ground state ^{3}He (eq 4).

$$[XC_6H_4{}^3He]^+ \xrightarrow{\text{ca. } 10^{-13}\text{ s}} XC_6H_4^+ + {}^3He \qquad (4)$$

Concerning the internal energy of the nucleogenic $XC_6H_4^+$ ions, it should be noted that the sudden nuclear transition generates ionic species whose geometry, reminiscent of the quasihexagonal skeleton of their XC_6H_5 precursors, does not correspond to the most stable structure of *relaxed* $XC_6H_4^+$ ions. The entity of such "deformation" energy can roughly be placed around 30 kcal mol^{-1}, in conformity with the results of theoretical calculations on isomeric $O_2NC_6H_4^+$ (Figure 1), $HOC_6H_4^+$ (Figure 2), and related species.[6g]

In conclusion, nuclear decay of a tritium atom in XC_6H_5 generates high yields (α = ca. 0.8) of labeled $XC_6H_4^+$ ions, initially in a σ-type singlet state, with an excess vibrational energy (up to ca. 30 kcal mol^{-1}) arising from the relaxation of their initially quasihexagonal structure to the most stable distorted geometry (Figures 1 and 2).

In regard to the available thermochemical data of substituted phenylium ions, Figure 3 reports a linear correlation (correlation coefficient = 0.985) between the stabilization energy in $XC_6H_4^+$ relative to the unsubstituted phenylium ion, expressed by the enthalpy change of the isodesmic reaction 5, as a function of the Hammett σ_p substituted constants.[18]

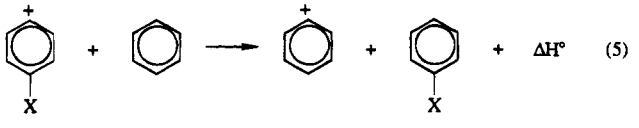

(5)

The heat of formation of p-$O_2NC_6H_5^+$ is known to be 283 kcal mol^{-1},[19] while that of p-$NCC_6H_4^+$ is derived from the correlation of Figure 3 to be ca. 316 kcal mol^{-1}. From the relative stability of isomeric $O_2NC_6H_4^+$ ions, obtained from the MP2/6-31G*//6-31G* calculations (Figure 1), the heat of formation of m- and o-$O_2NC_6H_4^+$ is derived as 283 and 293 kcal mol^{-1}, respectively. Similarly, the heat of formation of m- and o-$NCC_6H_4^+$ is estimated to range around 316 and 326 kcal mol^{-1}, respectively. The heat of formation of p-$HOC_6H_4^+$ is inferred from the linear correlation of Figure 3 to be ca. 219 kcal mol^{-1}. According to the MP2/6-31G*//6-31G* stability order reported in Figure 2, the ΔH_f's of m- and o-$HOC_6H_4^+$ are estimated to be ca. 215 and 226 kcal mol^{-1}, respectively.[20]

The $O_2NC_6H_4^+$ Reaction Pattern. In the discussion of the $O_2NC_6H_4^+$ reaction pattern toward the selected nucleophiles, it is convenient to consider first the results obtained in liquid CH_3OH, whose features appear to fit into the familiar picture of classical arenediazonium salts decomposition in the same solvent.[1,3] In these systems, in fact, the predominant products are isomeric nitroanisoles (Table 1), whose formation is ascribed to the attack of singlet $XC_6H_4^+$ ions on a lone pair of CH_3OH, yielding the corresponding methylaryloxonium ions **1** (eq 6; X = NO_2).

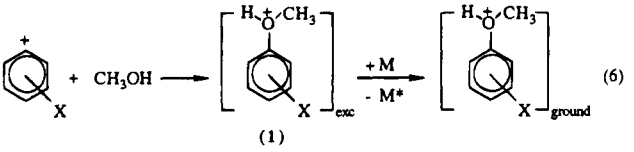

(6)

Intermediates **1**, excited by the exhothermicity of their formation process ($-\Delta H°$ (kcal mol^{-1}) = 62 *(para)*; 67 *(meta)*),[21] undergo collisional quenching with the M = CH_3OH molecules, very effective in liquid systems, and exothermic deprotonation by CH_3OH ($-\Delta H°$ (kcal mol^{-1}) $\approx$ 12 (*para*), 9 (*meta*))[22] to yield the observed nitroanisole products (eq 7; X = NO_2).

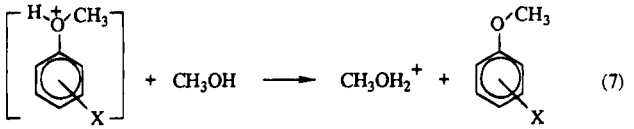

(7)

Alternatively, intermediates **1** may undergo exothermic nucleophilic displacement at their methyl group by CH_3OH with formation of tritiated nitrophenols ($-\Delta H°$ (kcal mol^{-1}) = ca. 27 (*para*), ca. 22 (*meta*)) (eq 8).

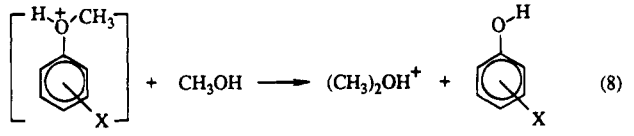

(8)

Despite their higher exothermicity, the substitution processes 8 are overwhelmed in liquid CH_3OH by the competing deprotonation reactions 7, as demonstrated by the predominant yield of nitroanisoles (94%) with respect to nitrophenols (3%). Fast cooperative deprotonation by several CH_3OH molecules in the liquid cage of **1** as well

(18) Hansch, C.; Leo, A.; Taft, R. W. *Chem. Rev.* **1991**, *91*, 165.
(19) Lias, S. G.; Bartmess, J. E.; Liebman, J. F.; Holmes, J. L.; Levin, R. D.; Mallard, W. G. *J. Phys. Chem. Ref. Data* **1988**, *17*, Suppl. 1.
(20) Grandinetti, F.; Speranza, M. *Chem. Phys. Lett.* **1994**, *229*, 581.
(21) These enthalpy changes, valid for gas phase processes at 298 K, have been calculated from the heats of formation of *para* (ref 19) and *meta* $O_2NC_6H_4^+$ (ΔH_f = 283 kcal mol^{-1}) (Figure 3) and from those of the corresponding oxonium intermediates **1** (X = NO_2) (ΔH_f (kcal mol^{-1}) = ca. 175 *(para)*; ca. 173 *(meta)*) estimated by assuming that the effect of the *para* and *meta* NO_2 group on the proton affinity of the oxygen atom of anisole (PA = 197 kcal mol^{-1}; cf. Reynolds, C. H.; Dewar, M. J. S. *J. Am. Chem. Soc.* **1982**, *104*, 3244) is equal to that on the stability of benzyl cation (Chung, D. S.; Kim, C. K.; Lee, B. S.; Lee, I. *Tetrahedron* **1993**, *49*, 8359). The exothermicity of the first step of eq 6 can amount to up to ca. 100 kcal mol^{-1} by considering the "deformation" energy of nucleogenic $XC_6H_4^+$ ions. In liquid CH_3OH, the exothermicities of reactions 6 and 7 can be slightly modified by the differential solvation energies of the involved species.
(22) These values arise from the difference between the proton affinity of CH_3OH (PA = 181.7 kcal mol^{-1}; Szulejko, J. E.; McMahon, T. B. *J. Am. Chem. Soc.* **1993**, *115*, 7839) and that on the etheral oxygen of *para* (PA = ca. 170 kcal mol^{-1}) and *meta* nitroanisole (PA = ca. 173 kcal mol^{-1}) estimated according to ref 21.

as the presence of substantial activation barriers in the displacement processes 8 may account for the largely different kinetics of reactions 7 and 8.

A similar pattern is operative in gaseous CH_3OH, with demethylation reactions 8 progressively prevailing over proton transfer 7 by decreasing the CH_3OH partial pressure. This behavior is indicative of both deprotonation reactions 7 sped up by clustering of CH_3OH molecules on **1** and of a more pronounced activation barrier associated to the displacement processes 8. Increasing the M = CH_3OH partial pressure (eq 6) favors collisional thermalization of excited **1**'s and, therefore, their lowest-activation energy deprotonation pathway 7.

The isomeric composition of tritiated nitranisoles and nitrophenols from liquid and gaseous CH_3OH samples does not match that expected from the initial tritium distribution in the starting $O_2NC_6H_5$ molecule (*ortho*, 40%; *meta*, 40%; *para*, 20%). In particular, while the ratio between the combined yields of *m*- and *p*-$O_2NC_6H_4OR$ (R = H, CH_3) reflects approximately the 2:1 ratio of their *m*- and *p*-$O_2NC_6H_4^+$ precursors under all conditions, the relative yields of *o*-$O_2NC_6H_4OR$ halves in liquid CH_3OH and practically zeroes in gaseous CH_3OH. Similarly, the *ortho* isomer is absent among the labeled $O_2NC_6H_4Cl$ products from the gaseous CH_3Cl samples, whose distribution is characterized by *meta*:*para* ratios close to 2.

Few hypotheses can be proposed which account for *all* the experimental evidences. A first explanation rests on the conceivable isomerization of the less stable *o*-$O_2NC_6H_4^+$ isomer (Figure 1) into the more stable *meta* and *para* isomers within a time which must be short relative to the collision time with gaseous CH_3Y (Y = OH, Cl) ($\leq 2.6 \times 10^{-11}$ s)[23] and comparable to that in liquid CH_3OH (ca. 10^{-14} s). Within this framework, the isomerization frequency of *o*-$O_2NC_6H_4^+$ should approach that typical of a bond vibration and, hence, involve negligible free energy barriers, if any. This requirement is in contrast with the typical behavior of strictly related arylium ions whose isomeric interconversion involve substantial activation free energies, e.g., phenylium[6b] and tolylium ions.[6d]

A more plausible rationale involves intramolecular electron transfer from a NO_2 lone pair to the formally vacant orbital of *o*-$O_2NC_6H_4^+$.

The vertical transition is made accessible in the "deformed" geometry of nucleogenic *o*-$O_2NC_6H_4^+$ by the proximity of the O lone pair and the empty sp^2 C orbital (cfr. structure **A'** in Figure 1). In this way, the structurally relaxed biradicalic structure **2I** is obtained (eq 9),

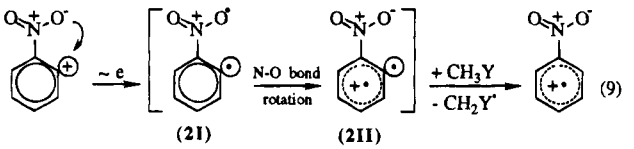

wherein extensive electron reshuffling from the ring π-system to the O atom to give **2II** is allowed by simple N−O bond rotation. It should be noted that direct electron transfer from the ring π-system of singlet *o*-$O_2NC_6H_4^+$ to the orthogonal vacant sp^2 orbital would hardy take place since it proceeds *via* a symmetry-forbidden intersystem crossing, while it appears as a very efficient (ca. 10^{14} s^{-1}) process since it is mediated by intervention of structure **2I**.

The ultimate fate of **2II** complies with the general behavior of biradicalic species, which readily abstract a H atom from CH_3OH or CH_3Cl (CH_3Y in eq 9) yielding the nitrobenzene radical cation. This, in turn, may either neutralize to a $O_2NC_6H_4H$ product undistinguishable from the starting multitritiated nitrobenzene (path a in eq 10) or combine with the $^{\bullet}CH_2Y$ (Y = OH) radical in

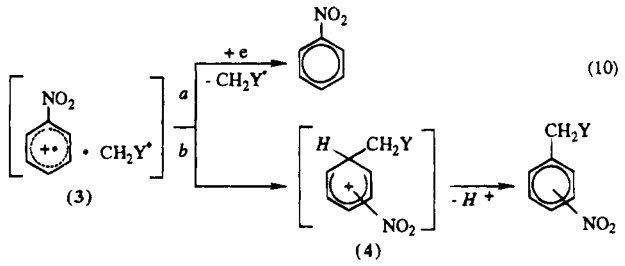

the encounter complex **3**, yielding the isomeric arenium intermediates **4** (path b of eq 10) and, eventually, the neutral $O_2NC_6H_4CH_2Y$ derivatives (Table 1).

According to the spin distribution in the nitrobenzene radical cation, the *meta* isomer of **4** should be preferentially formed as indeed verified from the slight predominance of the *meta* isomer among the $O_2NC_6H_4CH_2OH$ products. This distribution can, however, be somewhat altered by superimposition of direct insertion of singlet $O_2NC_6H_4^+$ into a CH bond of CH_3OH, a process which has been already observed with nucleogenic phenylium ion in liquid CH_3OH.[6b]

The $NCC_6H_4^+$ Reaction Pattern. In compliance with the general reaction pattern outlined in sequence 6 → 7, decay of NCC_6H_5 in methanol and methyl halides leads to the predominant formation of the corresponding labeled methoxybenzonitriles and halobenzonitriles (Table 2).

The isomeric composition of methoxybenzonitriles from CH_3OH samples and bromobenzonitriles from CH_3Br reflects approximately that expected from the initial tritium distribution in the starting NCC_6H_5 molecule (*ortho*, 40%; *meta*, 40%; *para*, 20%). This observation, which quite departs from the $O_2NC_6H_4^+$ reactivity model, witnesses the considerable difficulty of singlet *o*-$NCC_6H_4^+$ to convert readily into a biradicalic configuration by a process analogous to eq 9. This is likely due to the relatively large distance between the π and n orbitals of the CN moiety and the formally vacant orbital in *o*-$NCC_6H_4^+$, which prevents efficient electron transfer.

Along this line, the remarkable difference in the isomeric distribution of NCC_6H_4Y from gaseous CH_3Y (Y = F, Cl, Br) is to be ascribed to a different fate of their $[NCC_6H_4YCH_3]^+$ precursor intermediates in the corresponding medium. Once the operation of extensive intramolecular interconversion among the $[NCC_6H_4YCH_3]^+$ isomers is excluded on the grounds of previous convincing evidence on strictly related systems,[6c] the different fate of the $[NCC_6H_4YCH_3]^+$ in CH_3Y must be necessarily attributed to the specific nature of the gaseous nucleophile. In CH_3F, in fact, while *o*-NCC_6H_4F is formed in barely detectable amounts, the corresponding *meta* and *para* isomers are produced in abundant 2:1 proportions together with significant yields of *o*-$CH_3NHCOC_6H_4F$.

(23) Estimated from the collision rate constant between the $XC_6H_4^+$ ion and the CH_3Y molecule, calculated according to the ADO theory (Su, T.; Bowers, M. T. *Int. J. Mass Spectrom. Ion Phys.* **1973**, *12*, 347; **1975**, *17*, 211).

The exclusive formation of this *ortho* amide, in the absence of its other isomers, denotes its origin from the *ortho* fluoronium intermediate **5** (Y = F) to the expenses of the *o*-NCC_6H_4F product. A conceivable pathway (eq 11) involves exothermic methyl group transfer from F to

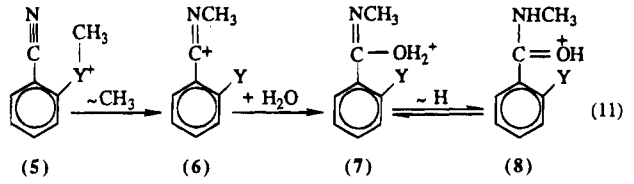

(5) (6) (7) (8) (11)

CN of **5**,[24] yielding the carbenium ion **6** which is stable enough in the reaction medium to be intercepted by all the nucleophilic impurities present in the gaseous mixture or formed from its radiolysis. Among these, a major one is H_2O which is known to rapidly add to iminocarbenium ions, such as **6**, yielding oxonium intermediates, such as **7** and **8**,[25] which produce *o*-$CH_3NHCOC_6H_4F$ by deprotonation. Therefore, taking into account that H_2O probably intercepts only a fraction, if a major one, of intermediates **6** and, hence, considering the combined yield of the *ortho* fluorinated products of Table 2 as reflecting in part the abundance of their common *o*-$NCC_6H_4^+$ precursor, the reaction pattern arising from the CH_3F systems conforms well to that in CH_3OH and CH_3Br, wherein occurrence of sequence 11 is prevented by the higher stability of **5** (Y = OH, Br) and, when Y = OH, by its rapid proton transfer to CH_3OH.

Concerning the mechanism of the first step of sequence 11 (Y = F), rough thermochemical estimates[26] suggest that isomerization might proceed intramolecularly as well as by intervention of a second molecule of CH_3Y (eq 12).

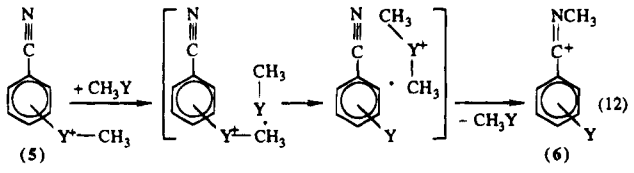

(5) (6) (12)

A hint into this question is provided from the analysis of the product composition in the CH_3Cl systems (Table 2), characterized by the unbalance of the isomeric NCC_6H_4Cl distribution in favor of the *meta* isomer and by the presence of significant amounts of both *o*- and *p*-$CH_3NHCOC_6H_4Cl$. In fact, formation of the latter product implies necessarily the operation of an intermolecular methyl-transfer mechanism proceeding via a CH_3Cl carrier. In this perspective, the exclusive formation of *ortho* and *para* amides reflects the favorable effect of the CN group at the *ortho* and *para* position of the corresponding precursors **5** (Y = Cl, eq 12) in promoting methyl group transfer to the CH_3Cl carrier.[27]

The failure to detect formation of *p*-$CH_3NHCOC_6H_4F$ in the CH_3F decay systems suggests that a similar effect seems much attenuated in intermediates **5** (Y = F), where the fluoronium center is expected to offer more resistance than the chloronium one in **5** (Y = Cl) to the π-acceptor CN substituent. It follows that, in these systems, CH_3F is inadequate as a methyl group carrier in eq 12 (Y = F), and therefore, formation of *o*-$CH_3NHCOC_6H_4F$ mainly involves an intramolecular mechanism.

The Reaction Patterns of $XC_6H_4^+$ (X = Cl, Br). In analogy with the behavior of the singlet $NCC_6H_4^+$ ion in liquid CH_3OH, nucleogenic $XC_6H_4^+$ (X = Cl, Br) ions efficiently add to a lone pair of CH_3OH, yielding the corresponding methylaryloxonium ion **1** (X = Cl, Br) (eq 6). Excited intermediates **1**[28] undergo effective collisional quenching by the M = CH_3OH molecules in competition with their deprotonation to the observed haloanisoles (eq 13).[29] In gaseous CH_3OH, coordination of a sufficient

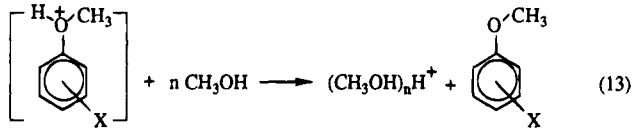

(13)

number of CH_3OH molecules around the proton of **1**, necessary for deprotonation 13,[28] competes with direct nucleophilic displacement at the methyl moiety of **1** by CH_3OH yielding the corresponding halophenols (eq 8) (Tables 3 and 4). The relatively slow displacement reaction 8 is, in fact, superseded again by fast deprotonation of **1** when cooperative deprotonation 13 by gaseous CH_3OH molecules is replaced by the much more efficient proton transfer from **1** to a $(CH_3)_3N$ molecule (PA = 225.1 kcal mol^{-1}).[19] The powerful $(CH_3)_3N$ base effectively

(24) The proton affinity of the CN moiety in C_6H_5CN is ca. 30 kcal mol^{-1} higher than that of the F atom in fluorobenzene (cf. Lau, Y. K.; Kebarle, P. *J. Am. Chem. Soc.* **1976**, *98*, 7452. Hrusak, J.; Schröder, D.; Weiske, T.; Schwarz, H. *J. Am. Chem. Soc.* **1993**, *115*, 2015 and references therein). Within the reasonable assumption that methyl cation affinities correlate well with the corresponding proton affinities and considering the different electronic effect of the CN group in **5** and the F substituent in **6** (eq 11), it is conceivable that the first step of sequence 11 is exothermic by over 30 kcal mol^{-1}.

(25) (a) Cacace, F.; Ciranni, G.; Giacomello, P. *J. Am. Chem. Soc.* **1982**, *104*, 2258. (b) Attinà, M.; Cacace, F.; Ricci, A. *Angew. Chem., Int. Ed. Engl.* **1991**, *30*, 1457.

(26) *Ab initio* theoretical calculations indicate that the proton affinity of the F atom of fluorobenzene (PA = 149.5 kcal mol^{-1}; Hrusak, J.; Schröder, D.; Weiske, T.; Schwarz, H. *J. Am. Chem. Soc.* **1993**, *115*, 2015) is comparable to that of CH_3F (PA = 145 kcal mol^{-1}; ref 19). By assuming a strict correlation between the proton and the methyl cation affinities of organic halides (McManus, S. P. *J. Org. Chem.* **1982**, *47*, 3070) and by considering the destabilizing effect of the CN group in **5**, the second step of sequence 12 (Y = F, Cl) might be thermochemically allowed.

(27) Processes similar to eqs 11 and 12 may take place within the $[O_2NC_6H_4ClCH_3]^+$ intermediates as well. In these systems, however, conceivable exothermic methyl group transfer from Cl to the NO_2 moiety leads to an oxonium ions whose evolution can proceed exclusively via methyl group transfer to a suitable acceptor, again yielding $O_2NC_6H_4Cl$.

(28) A reaction enthalpy of ca. −79 kcal mol^{-1} has been estimated for the first step of sequence 6, when X = OCH_3. This value, which refers to a gas-phase reaction at 298 K, has been calculated by using the heat of formation of $XC_6H_4^+$, as arising from the correlation of Figure 3, and that of the corresponding oxonium ion **1** (X = OCH_3) (ca. 100 kcal mol^{-1}), derived within the assumption that the effect of the *para* X group on the proton affinity of the oxygen of anisole (PA = 197 kcal mol^{-1}; cf.Reynolds, C. H.; Dewar, M. J. S. *J. Am. Chem. Soc.* **1982**, *104*, 3244) is equal to that on the stability of benzyl cation (Chung, D. S.; Kim, C. K.; Lee, B. S.; Lee, I. *Tetrahedron* **1993**, *49*, 8359). Comparison of the so-calculated reaction enthalpy with that involving *para* $O_2NC_6H_4^+$ ions (ca. −62 kcal mol^{-1}) suggests that minor conjugative effects of X in $XC_6H_4^+$ fully develop in their corresponding derivatives **1**. Along this line, the exothermicity of the first step of sequence 6 ranges from −62 to −79 kcal mol^{-1}, when X = Cl, Br, and OH. These values can be further lowered by ca. 30 kcal mol^{-1}, if the "deformation" energy of the nucleogenic $XC_6H_4^+$ is considered. In liquid CH_3OH, the estimated enthalpy changes of eqs 6 and 7 may be slightly modified by the differential solvation energies of the involved species.

(29) According to the heat of formation of **1**, estimated in ref 28 as ca. 100 kcal mol^{-1} when X = OCH_3, the gas phase proton-transfer reaction 7 for X = OCH_3 is endothermic by ca. 28 kcal mol^{-1}. A similar endothermicity can be expected when X = Cl, Br, or OH. However, deprotonation 7 may well occur if the oxonium ion **1** is still excited or if preliminary coordination of several CH_3OH molecules ($n > 1$) around the proton of **1** (eq 13), a process favored in the liquid phase, takes place (cf. Grismrud, E. P.; Kebarle, P. *J. Am. Chem. Soc.* **1973**, *95*, 7939. Hiraoka, K.; Grimsrud, E. P.; Kebarle, P. *J. Am. Chem. Soc.* **1974**, *96*, 3359). Demethylation reaction 8 is estimated to be ca. 18 kcal mol^{-1} endothermic.

Table 7. Gas-Phase Deprotonation vs Demethylation Ratio of 1

	[$XC_6H_4OCH_3$]/[XC_6H_4OH]				
X	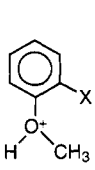	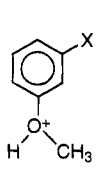	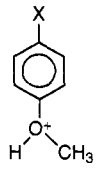	CH_3OH (Torr)	source
NO_2		1.4	1.3	65	this work
		0.9	0.6	50	this work
		0.5	0.7	20	this work
CN	very large	very large	very large	65–5	this work
H	24.0	24.0	24.0	65	ref 6b
	19.0	19.0	19.0	55	ref 6b
	6.1	6.1	6.1	20	ref 6b
	4.0	4.0	4.0	5	ref 6b
Cl	3.8	7.3	2.7	65	this work
	0.9	4.9	2.0	5	this work
Br	1.1	2.7	1.2	65	this work
	0.9	2.3	1.0	30	this work
	1.2	5.2	1.5	10	this work
	1.3	5.2	1.7	5	this work

competes with CH_3OH not only in deprotonating **1**, but also in intercepting their $XC_6H_4^+$ precursors. Accordingly, the ca. 20% depletion of the absolute yields of $XC_6H_4OCH_3$, observed in 65 Torr CH_3OH in the presence of 10 Torr $(CH_3)_3N$ (Tables 3 and 4), besides demonstrating the ionic origin of the decay products, points to an efficiency for eq 6 (X = Cl, Br) similar to that of $XC_6H_4^+$ trapping by the very strong $(CH_3)_3N$ nucleophile ($k(CH_3OH)/k((CH_3)_3N)$ = ca. 0.7).

The isomeric composition of labeled haloanisoles from liquid CH_3OH and gaseous CH_3OH (65 Torr), in the presence of 10 Torr of $(CH_3)_3N$, reflects approximately that expected from the initial tritium distribution in the starting XC_6H_5 (X = Cl, Br) molecules (*ortho*, 40%; *meta*, 40%; *para*, 20%) (Tables 3 and 4). In gaseous CH_3OH in the absence of added $(CH_3)_3N$, the isomeric distribution of haloanisoles and halophenols appreciably diverges from the *ortho*:*para*:*meta* = 2:2:1 composition of their common $XC_6H_4^+$ precursors. Nevertheless, this distribution is approximately restored if the combined *ortho*:*para*:*meta* ratios of the two families of products, i.e., *ortho*:*meta*:*para* = (1.7–2.2):(1.9–2.3):1.0, are considered.

The different isomeric distribution of haloanisoles and halophenols as a function of the CH_3OH partial pressure is thought to arise from the effect of the substituent X on the relative extent of the competing processes 13 and 7 (Table 7). The powerful σ- and π-electron withdrawing NO_2 group in isomeric intermediates **1** (X = NO_2) makes thermodynamically accessible both competing processes 13 (n = 1) and 7 and facilitates inversion of configuration of the methyl moiety of **1** in the displacement process 8. It follows that the relative extent of 13 (n = 1) vs 8 is determined essentially by statistics (efficiency ratio = ca. 1), although CH_3OH clustering around **1** (n > 1), favored at high CH_3OH pressures, somewhat enhances deprotonation over demethylation. With X = CN, rough thermochemical estimates indicate that deprotonation 13 by a single CH_3OH molecule (n = 1) is slightly endothermic ($\Delta H°$ = ca. +7 kcal mol^{-1}) and becomes exothermic by intervention of a second CH_3OH molecule (n = 2).[28,29] The competing demethylation 8 is instead exothermic by ca. 9 kcal mol^{-1}. In consideration of the substantial activation barrier involved in the inversion of the CH_3 configuration in eq 8, it is plausible that rapid proton transfer 13 (n = 2) within the encounter complex prevails over the competing substitution 8. Exclusive formation of isomeric $XC_6H_4OCH_3$ (X = CN) ensues.

With X = H, *m*-Cl, and *m*-Br, deprotonation 13 by a single CH_3OH molecule is estimated to be ca. 15 kcal mol^{-1} endothermic, whereas demethylation 8 is almost thermoneutral. Furthermore, the activation barrier involved in the displacement process 8 is expected to increase by increasing the electron-donating character of the substituent X. It follows that, in these systems, deprotonation by several CH_3OH molecules (eq 13, $n \geq 2$) predominates over demethylation 8. With X = *o*-Cl, *p*-Cl, o-Br, and *p*-Br, the π-donating properties of the substituent make both deprotonation 13 by a single CH_3OH molecule and the competing demethylation reaction 8 markedly endothermic.[29] In this case, deprotonation 13 requires assembling around **1** of organized clusters of many CH_3OH molecules, favored at the highest CH_3OH pressures. It follows that interception of **1** by highly nucleophilic impurities, present in the decay mixture or formed from its radiolysis, may effectively compete with deprotonation,[6d,9] yielding significant amounts of XC_6H_4OH, besides $XC_6H_4OCH_3$.

The observation that the isomeric composition of the neutral derivatives of **1** (X = Cl, Br; Tables 3 and 4) reflects closely that of their $XC_6H_4^+$ precursors denotes that singlet $XC_6H_4^+$ ions, at variance with the phenylium and tolylium ion analogues,[6,9] do not exhibit any net tendency to interconvert by intramolecular 1,2-hydron shifts. A further evidence is provided by the approximate *ortho*:*meta*:*para* = 2:2:1 distribution of XC_6H_4Y products, recovered in the gaseous methyl halide CH_3Y systems (Tables 3 and 4).

The $HOC_6H_4^+$ Reaction Pattern. In the discussion of the results concerning decay of ring-multitritiated phenol in liquid CH_3OH, it is necessary to define first the behavior of the labeled substrate in the reaction medium. A first question concerns the possibility that, during the prolonged decay storage (12–16 months), slow isotopic exchange of ring-multitritiated phenol by liquid CH_3OH may somewhat alter the tritium atom distribution in its aromatic ring and, thus, modify with time the isomeric distribution of the nucleogenic $HOC_6H_4^+$ ion family.

It is well established that extensive ring-hydrogen exchange in phenol can be promoted by strong acids and bases.[30] With both catalysts, exchange involves exclusively the hydrogens *ortho* and *para* to the substituent, besides the OH hydrogen itself. The *meta* hydrogens remain, instead, untouched even after prolonged and intense heating. Strong acids and bases are absent in the liquid HOC_6H_5/CH_3OH decay mixtures, the most "acidic" species being the labeled phenol itself, which is highly reluctant to lose its OH proton (pK_a = 14.46 at 25 °C)[31] and, therefore, to catalyze any appreciable ring-tritium exchange. Formation of significant yields of *p*-$HOC_6H_4OCH_3$ in the expected proportion relative to *meta* (Table 5) provide experimental support against appreciable ring-tritium exchange in the HOC_6H_5 molecule during the storage period.

Another relevant question refers to solvation of HOC_6H_5 in liquid CH_3OH, since nucleogenic $HOC_6H_4^+$ ions are

(30) Small, P. A.; Wolfenden, J. H. *J. Chem. Soc.* **1936**, 1811.
(31) Rochester, C. H.; Rossall, B. *J. Chem. Soc., Faraday Trans.* **1969**, *65*, 1004.

generated initially within the same solvation shell of their precursor. Phenol, in liquid CH_3OH at room temperature, is completely associated,[32] according to the predominant structure **9** (eq 14).[33] Interchange between

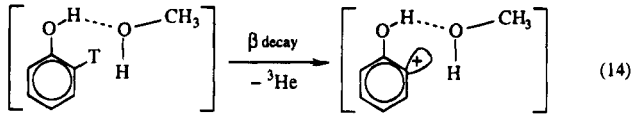

(9) (10) (14)

the OH protons of **9** is a relatively fast process involving an activation barrier of 5 ± 1 kcal mol^{-1}.[33] In this framework, it is reasonable to interpret the relatively low yield of *o*-$HOC_6H_4OCH_3$ (5%) formed in the liquid CH_3OH systems as due to fast prototropic rearrangement in the "distorted" structure **10**, prior to rotational relaxation of the organized CH_3OH cluster (eq 15). The very stable

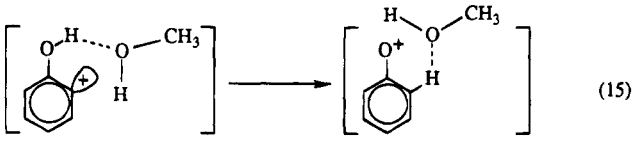

(10) (11) (15)

phenoxenium ion **11** is formed (structure **G** in Figure 2), whose fate is to either undergo CH_3OH addition at its *ortho* (minor) or *para* (major) positions yielding eventually the corresponding methoxyphenols,[34] or exothermically abstract a hydride ion from CH_3OH producing HOC_6H_4H, indiscriminable from the starting multitritiated phenol.[35] Sequence 14 → 15 is much less favored when decay involves *meta* and *para* T atoms in HOC_6H_5, owing to the larger distance between its OH moiety and the incipient vacant orbital. As a result, an isomeric distribution of labeled methoxyphenols is obtained from liquid CH_3OH, characterized by a significant depletion of the *ortho* isomer and by the formation of the *meta* and *para* isomers, in the expected ca. 2:1 ratio.

In gaseous CH_3Cl, the isomeric composition of the labeled chlorophenol products is found to depend upon the CH_3Cl partial pressure (Table 5). At $P(CH_3Cl) > 100$ Torr, an *ortho*:*meta*:*para* = (1.8–2.5):(1.9:2.3):1.0 ratio is obtained, approximately reflecting the initial *ortho*:*meta*:*para* = 2:2:1 distribution of their $HOC_6H_4^+$ precursors. The chlorophenols' composition changes significantly at $P(CH_3Cl) < 100$ Torr becoming *ortho*:*meta*:*para* = 1.0:1.3:1.0 at 10 Torr. This trend can hardly be traced to rearrangement of the halonium ions **12** and must arise, in compliance with the behavior of the $XC_6H_4^+$ (X = H, CH_3) analogues,[6,9] from isomerization of gaseous $HOC_6H_4^+$ ions before their trapping by CH_3Cl (eq 16).

Best fit of the experimental results of Table 5 with the rate equations, derived according to the isomerization sequence 16, provides an estimate of the relevant phenomenological *k* values, as reported in Table 8. The *meta* > *para* > *ortho* $HOC_6H_4^+$ stability order (Figure 2) accounts for the net depletion of the *ortho* isomer by

Table 8. Phenomenological $XC_6H_4^+$ Isomerization Rate Constant ($\times 10^{-9}$ s^{-1})

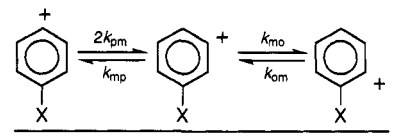

substituent X	k_{pm}	k_{mp}	k_{mo}	k_{om}	source
H	0.3	0.3	0.3	0.3	ref 6b
CH_3	2.7	2.6	2.8	3.8	ref 6d
OH	0.6	1.0	1.1	1.5	this work

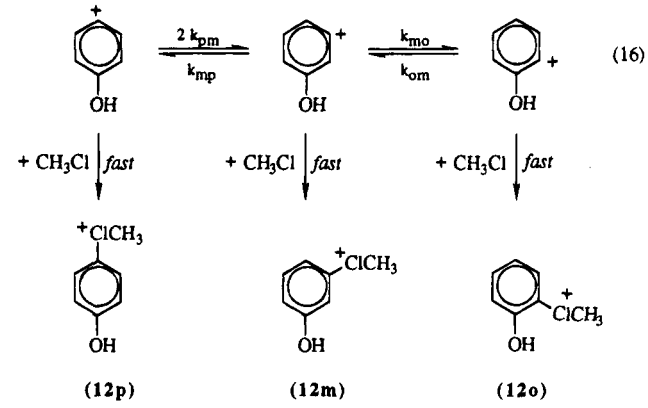

(12p) (12m) (12o) (16)

increasing the ion lifetime (Table 5) while the net increase of the *para* relative yield, within the ion lifetime window open to the decay experiments, points to interconversion kinetics essentially governed by entropic factors within "deformed" $HOC_6H_4^+$ ions.[36]

According to the relevant $HOC_6H_4OCH_3$ distribution (*ortho* (0.6:1.1); *meta* (<0.1); *para* 1.0) (Table 5), the isomerization sequence 16 is obscured in the gaseous CH_3OH samples by parasitic processes involving the CH_3OH nucleophile and leading to a marked decrease of the product yields mainly to the expenses of the *meta* isomer. A rationale for this observation can be found in the pronounced gas-phase Brønsted acid character of *m*-$HOC_6H_4^+$, absent in its *ortho* and *para* isomers, due to the extensive p – π conjugative stabilization in its conjugate base **13m** (eq 8).[20]

Indeed, *ab initio* calculations (Figure 2) indicate that gaseous "deformed" *m*-$HOC_6H_4^+$ at 298 K ($\Delta G°_{298}$ = ca. 168 kcal mol^{-1} for eq 17) is ca. 6 kcal mol^{-1} more acidic than $CH_3OH_2^+$ ($\Delta G°_{298}$ = 174 kcal mol^{-1}).[19] On the contrary, gaseous $CH_3OH_2^+$ is ca. 8 and 12 kcal mol^{-1} more acidic than "deformed" *o*- and *p*-$HOC_6H_4^+$ ions, respectively. It follows that, in the excited encounter complex between "deformed" *m*-$HOC_6H_4^+$ ion and CH_3OH, the entropy-favored transfer of the HO proton of the

(32) Aarna, I. A.; Melder, L. *Tr. Tallinsk. Politekhn. Inst. Ser. A* **1960**, *185*, 304.

(33) (a) Gränacher, J. *Helv. Phys. Acta* **1958**, *31*, 734. (b) Némethy, G.; Ray, A. *J. Phys. Chem.* **1973**, *77*, 64.

(34) Endo, Y.; Shudo, K.; Okamoto, T. *J. Am. Chem. Soc.* **1982**, *104*, 6393.

(35) According to the *ab initio* data of Figure 2, *para* $HOC_6H_4^+$ (ΔH_f = ca. 219 kcal mol^{-1}) is 22 kcal mol^{-1} less stable than phenoxenium ion $C_6H_5O^+$, whose formation enthalpy at 298 K can be estimated as ca. 197 kcal mol^{-1}. Accordingly, hydride-ion transfer from the methyl group of CH_3OH to the oxygen of $C_6H_5O^+$ is exothermic by ca. 6 kcal mol^{-1}, in the gas phase.

(36) The relatively high *k* values for $HOC_6H_4^+$ isomerization 16 (Table 8) are in apparent contrast with the recent observation of a significant stability for the same species under FT-ICR conditions (ref 20). It should be realized, however, that the $HOC_6H_4^+$ ions, generated in the FT-ICR source by CF_4-CIMS of the corresponding fluorophenols, share with the outgoing CF_4 the excess energy arising from the exothermicity of their formation process ($\Delta H° = -29$ kcal mol^{-1}) (ref 19). In addition, most of this excess energy is spread over all the degrees of freedom of the ion, while the "deformation" energy associated to the same nucleogenic species is initially localized around the positively charged ring carbon and its σ C–H and C–C neighbors. Thus, it is reasonable that the $HOC_6H_4^+$ ions formed in the FT-ICR source, despite their relatively long lifetime (several seconds at ca. 10^{-8} Torr), display a higher reluctance toward interconversion than nucleogenic $HOC_6H_4^+$ ions.

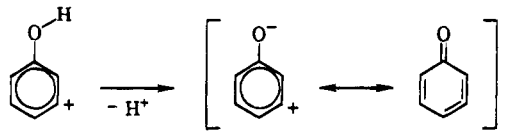

(13m) (17)

arylium ion to CH_3OH precedes addition 6. The same process is thermodynamically precluded to the *o*- and *p*-$HOC_6H_4^+$ isomers, which therefore follows predominantly the addition reaction 6.[37]

The fate of the conjugate base **13m** of the *m*-$HOC_6H_4^+$ Brønsted acid in gaseous CH_3OH is rather obscure. However, in consideration of the approximate *ortho*:*para* = ca. 1:1 ratio observed in the gaseous CH_3OH samples, closely matching that measured in the CH_3Cl systems under comparable conditions, it can be concluded that those conceivable aliquots of cumulene **13m** adding to CH_3OH would produce both *o*- and *p*-$HOC_6H_4OCH_3$ in comparable proportions (eq 18).[38]

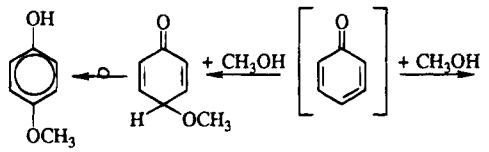

(13m)

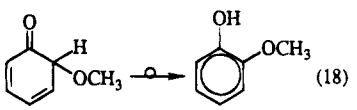

(18)

The $CH_3OC_6H_4^+$ Reaction Pattern. Nuclear decay of $CH_3OC_6H_5$ in liquid CH_3OH produces exclusively substantial amounts of dimethoxybenzenes (68%; Table 6). Their isomeric composition (*ortho*:*meta*:*para* = 35%:45%:20%) conforms approximately to that expected for their $CH_3OC_6H_4^+$ precursors (*ortho*:*meta*:*para* = 2:2:1). This distribution quite departs from that of the labeled $HOC_6H_4OCH_3$ (*ortho*:*meta*:*para* = 5%:69%:26%), obtained in the strictly related decay systems with $HOC_6H_4^+$ under the same conditions (Table 5), and attributed to sequence 14 → 15. Preferential assemblage of the anisole solvation shell in liquid CH_3OH through hydrogen-bonded structures like **15** (eq 19), rather than by the less stable structures **14** (analogous to **9** in eq 14), accounts for such a difference.

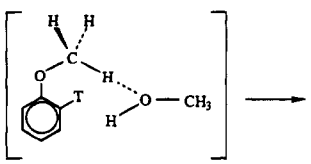

(14)

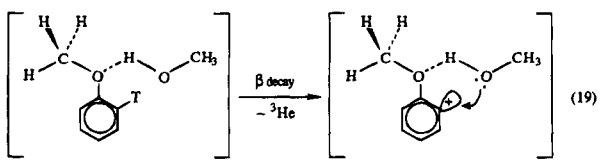

(15) (19)

In comparison with the liquid CH_3OH systems, decay of $CH_3OC_6H_5$ in gaseous CH_3OH and CH_3Cl mixtures leads to the formation of the corresponding dimethoxybenzenes and chloroanisoles, respectively, together with minor yields of phenol (in CH_3OH) and chlorobenzene (in CH_3Cl) (Table 6). The isomeric distributions of dimethoxybenzenes and chloroanisoles are characterized by the exceedingly low proportions of the *ortho* isomers (≤ 7%), becoming barely appreciable at the lowest system pressures (ca. 1% at P ≤ 50 Torr), whereas the *meta*:*para* (= 2.0−2.6):1.0 ratios remain essentially constant and close to the initial *meta*:*para* = 2.1 ratio of their $CH_3OC_6H_4^+$ precursors under all conditions. Depletion of the *ortho* isomers is counterbalanced by formation of phenol (in CH_3OH) and chlorobenzene (in CH_3Cl), in relative yields increasing by decreasing the nucleophile concentration.

This picture points to a fast isomerization process in *o*-$CH_3OC_6H_4^+$ preceding both its trapping by the nucleophile and its intramolecular isomerization to the *meta* and *para* isomers, which leads to the formation of phenol, in CH_3OH, and chlorobenzene, in CH_3Cl.

A plausible hypothesis, which finds close analogies with similar processes observed in mass spectrometry,[39] involves fast 1,4-hydride-ion transfer from the methyl group to the vacant ring orbital of singlet *o*-$CH_3OC_6H_4^+$, allowed in its "deformed" geometry by the proximity of the two centers (eq 20).

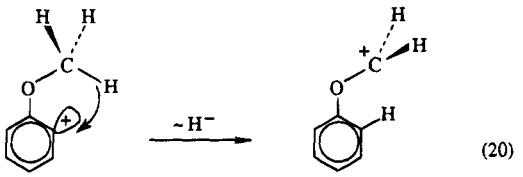

(16) (17) (20)

The process is analogous to that occurring in *o*-$O_2NC_6H_4^+$, where the oxygen lone-pair electrons, rather than the C−H σ-bond electrons of **16**, are involved. It represents a practicable route for "deformed" nucleogenic ions **16** to bypass comparatively slow structural relaxation.

The phenoxymethylium ion **17**, excited by the exothermicity of its formation process 20,[40] is nevertheless a rather stable species under the decay conditions, whose fragmentation is severely hampered by high endothermicities (ΔH° > 40 kcal mol^{-1}) and pronounced activation barriers.[39,41] It follows that a substantial fraction of excited **17** will be intercepted by the nucleophiles present in the gaseous mixture prior to fragmentation.

Formation of labeled phenol in the CH_3OH systems and of chlorobenzene in the CH_3Cl ones, besides from partial fragmentation of excited **17**,[41] is thought to arise from the common reaction network 21. Owing to their

(37) It should be noted that gas phase proton loss from nucleogenic $HOC_6H_4^+$ isomers to CH_3Cl is prevented since it is endothermic by at least 13 kcal mol^{-1} (ref 19).

(38) Johnson, R. P. *Chem. Rev.* **1989**, *89*, 1111.

(39) (a) Russell, D. H.; Freiser, B. S.; McBay, E. H.; Canada, D. C. *Org. Mass Spectrom.* **1983**, *18*, 474. (b) Molenaar-Langeveld, T. A.; Ingemann, S.; Nibbering, N. M. M. *Org. Mass Spectrom.* **1993**, *28*, 1167.

(40) By assuming that the heat of formation of phenoxymethylium ion **17** (ref 39) is equal to 153 kcal mol^{-1}, reaction 20 is exothermic by ca. 72 kcal mol^{-1}, if a relaxed *ortho* $CH_3OC_6H_4^+$ ion is involved, and by over 100 kcal mol^{-1}, if a "deformed" *ortho* $CH_3OC_6H_4^+$ is involved.

(41) The major fragmentation processes occurring in excited **17** is by loss of either CO or CH_2O. Extrusion of CO is accompanied by extensive ring opening and contraction, which would lead in the decay systems to nonaromatic labeled products. Loss of CH_2O would produce a phenylium ion, which, in CH_3OH, mainly yields labeled anisole, undistinguishable from the starting compound, and, in CH_3Cl, labeled chlorobenzene (refs 6, 9, and 39).

endothermicities ($\Delta H°$ (kcal mol^{-1}) = +29 (i) (A = H); +22 (i) (A = CH_3); +37 (ii) (A = CH_3; Nu = Cl)) occurrence of network 21 is favored at the lowest pressures, namely under conditions minimizing collisional quenching of the ionic intermediates involved (Table 6).

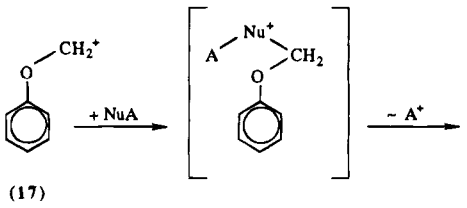

(17)

NuA = CH_3OH (A = H or CH_3)
CH_3Cl (A = CH_3)

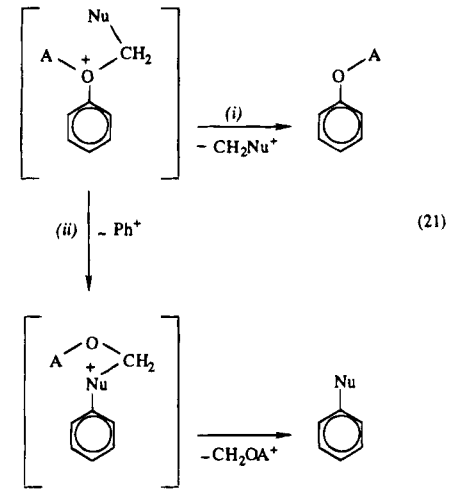

(21)

Conclusions

The results of the present study extend the analysis of the structure and the reactivity of free substituted phenylium ions outlined in previous investigations.[6,9] The reactivity picture of nuclear-decay formed arylium ions toward nucleophilic acceptors, such as methanol and methyl halides, in both gaseous and liquid phases conforms to a stable single-state electronic configuration. Singlet *o*-$O_2NC_6H_4^+$ rapidly converts into a biradicalic configuration by virtue of the proximity of a lone-pair orbital of the O of NO_2 to the formally vacant ring orbital. The same efficient intersystem crossing is instead prevented in *o*-$NCC_6H_4^+$ by unfavorable spatial arrangement of the involved orbitals. Occurrence of facile intersystem crossing in *o*-$O_2NC_6H_4^+$ does not necessarily imply a biradicalic ground state, since it may just reflect a facile charge dispersal from the σ to the π framework of the "deformed" ion, whose way back may be kinetically hindered by unfavorable entropy factors. The isomeric distribution of the decay products generally matches that of their $XC_6H_4^+$ precursors under all experimental conditions. It is concluded that, at variance with the behavior of $XC_6H_4^+$ (X = H, CH_3),[6,9] isomeric $XC_6H_4^+$ (X = NO_2, CN) ions do not exhibit any tendency to interconvert by intramolecular 1,2-hydrogen shifts, thus suggesting that the relevant activation barriers increase substantially in the presence of a powerful electron-withdrawing substituent on the aromatic ring. On the contrary, when X = H, CH_3, and OH excess internal energy in "deformed" nucleogenic $XC_6H_4^+$ allows extensive gas-phase intramolecular 1,2 ring-hydrogen shifts favoring the most stable isomeric forms. The relevant rate constants, reported in Table 7, indicate that ring-hydrogen migration is favored by σ-donating groups as well as by powerful π-donating substituents (X = OH). Observation of ring-hydrogen migrations in $CH_3OC_6H_4^+$ is complicated by the superimposition of a faster isomerization process involving exclusively the *ortho* isomer. In its "deformed" geometry, the proximity of the vacant ring orbital to the C-H σ bonds of the methyl moiety favors occurrence of a comparatively fast 1,4-hydride ion transfer prior to any other conceivable structural reorganization. In liquid CH_3OH, differential CH_3OH assemblage around the substituent of HOC_6H_5 and $CH_3OC_6H_5$ induces marked differences in the corresponding *o*-$XC_6H_4^+$ ions. Predominance of structures like **9** in HOC_6H_5 favors intermolecular prototropic migration yielding the phenoxenium ion **11**, whereas in $CH_3OC_6H_5$ the prevailing structures **15** allows rapid trapping of the corresponding $CH_3OC_6H_4^+$ ion by CH_3OH.

Acknowledgment. Financial support from Ministero dell'Università e della Ricerca Scientifica e Tecnologica (MURST) and from Consiglio Nazionale delle Ricerche (CNR) is gratefully acknowledged. We thank F. Grandinetti for his invaluable help in performing calculations and F. Cacace and G. Angelini for their interest in the present work.

JO941676D